

1 Global Ocean Data Set of Marine Aerosol Properties

2
3 Patricia K. Quinn¹, Timothy S. Bates², Derek J. Coffman¹, James E. Johnson², Lucia M. Upchurch², and
4 Hanna Best²

5
6 ¹NOAA Pacific Marine Environmental Laboratory, Seattle, WA, USA

7 ²Cooperative Institute for Climate Ocean and Ecosystem Studies (CICOES), University of Washington, Seattle, WA, USA

8
9 *Correspondence to:* Patricia K. Quinn (patricia.k.quinn@noaa.gov)

10
11 **Abstract.** NOAA's Pacific Marine Environmental Laboratory (PMEL) has made measurements of
12 aerosol chemical, microphysical, optical, and cloud nucleating properties onboard research cruises since
13 1991. The twenty-five cruises have covered all of the world's oceans -- the Pacific, Atlantic, Indian,
14 Arctic, and Southern. The result is the most comprehensive, publicly available database of aerosol
15 properties in the marine atmosphere to date. The database also contains gas-phase species (O₃, SO₂,
16 Radon, and dimethylsulfide (DMS), seawater species (DMS, NH₄⁺, NO₃⁻, and chlorophyll-a), and
17 meteorological parameters. Details of the cruises (locations, dates, and objectives), parameters measured,
18 instrumentation used, and data availability are provided here. Also included are PMEL's high-level major
19 findings and past usage of the data by others. The goal of this paper is to promote broader awareness of
20 the database to the atmospheric aerosol *in situ* measurement, satellite, and modelling communities. Data
21 are publicly available at NOAA's National Centers for Environmental Information (NCEI) data archive
22 (<https://www.ncei.noaa.gov/>). Links to the Digital Object Identifiers (DOIs) for each cruise are provided
23 herein.

24 25 **1 Introduction**

26
27 Aerosol particles influence Earth's radiation budget directly by scattering and absorbing incoming solar
28 radiation and indirectly by acting as cloud condensation nuclei (CCN) and impacting cloud properties
29 including reflectivity, lifetime, and spatial extent. The concentration and composition of aerosol particles
30 vary both geographically and temporally, leading to a wide range of local and global climate impacts.
31 Over oceans, aerosol particles have both continental and oceanic sources. Particles emitted from
32 continental sources, including fossil fuel combustion, biomass burning, dust, and biogenic emissions, can
33 be transported hundreds to thousands of kilometers over oceans either in the boundary layer or the free

34 troposphere (FT) (Clarke et al., 2013). Aerosol number and mass concentrations, chemical composition,
35 and optical and cloud-nucleating properties are impacted by transport events and vary with distance from
36 shore (Quinn et al., 2015). The ocean itself is a source of aerosol particles through wave-breaking at the
37 surface and subsequent bubble bursting (De Leeuw et al., 2011). In addition, marine vessel emissions also
38 contribute to the aerosol population over oceans, particularly in coastal regions and major shipping lanes
39 (Corbett et al., 2007). Marine aerosol is defined here as particles in the atmosphere over oceans regardless
40 of origin.

41
42 Observations of aerosol properties in the marine atmosphere are required to improve the accuracy of
43 model simulations of their radiative effects. Satellite observations provide broad spatial and temporal
44 coverage of the atmospheric aerosol burden over the world's oceans and reveal information about
45 seasonally persistent transport from continents. Examples include the transport of African dust westward
46 across the Atlantic every summer (Kaufman et al., 2005) and transport of Asian dust and pollution
47 eastward across the Pacific during the spring (Logan et al., 2010). While satellite observations have the
48 advantage of providing global coverage, *in situ* observations have the highest level of accuracy available
49 to constrain radiative forcing and reduce uncertainties in forcing estimates (Li et al., 2022). As such, *in*
50 *situ* measurements provide detailed information about the processes controlling variability in aerosol
51 properties due to complex particle and gas phase precursor sources, transport pathways, and removal
52 processes.

53
54 Cruises conducted since 1991 by PMEL cover all of the world's oceans providing the most
55 comprehensive, publicly available global database to date of marine aerosol microphysical, chemical,
56 optical, and cloud-nucleating properties. The data set is unique in that standardized methods and sampling
57 protocols were employed including particle size cuts at a common relative humidity upstream of
58 instrumentation and particle collection devices. This approach eliminates biases in the data and allows for
59 direct comparison of measured regional properties between cruises. The global nature of the data set
60 makes it well-posed to address current scientific priorities including reducing uncertainties in aerosol

61 radiative forcing and links between ocean biology and climate. The details provided here describing the
62 measurements in depth are intended to increase the usability of the data.

63

64 The cruises were process oriented geared toward understanding the effects of formation, emission,
65 atmospheric transformation and removal on aerosol properties. Some of the cruises were conducted
66 during the time of the year when a targeted plume was expected to be most pronounced. For those cruises,
67 the range of reported values most likely is skewed toward higher values that are typical of seasonally
68 maximum plumes. In addition, reported variability in the data are based on a snapshot during the short-
69 lived campaigns. Objectives are described and references are cited to provide context for each cruise.

70

71 This paper describes the measurements in detail, the data that are available for each cruise, PMEL's major
72 findings, and data usage by others. The goal is to provide information about data availability and to
73 advance the widespread use of the data to the atmospheric aerosol *in situ* measurement, satellite, and
74 modelling communities. Sect. 2 describes the cruises and Sect. 3 describes the methods. PMEL's major
75 findings are summarized in Sect. 4., data usage by others in Sect. 5, and a brief summary in Sect. 6. Data
76 availability is described in Sect. 7.

77

78 **2 Global Ocean Cruises**

79

80 Ship tracks of PMEL's cruises between 1991 and 2020 are shown in Figure 1. A list of the cruises with
81 start and stop dates, departure and arrival ports, location, and relevant references is provided in Table 1.
82 A complete list of instrumentation on each cruise is presented in Section 3. Each cruise is briefly described
83 in the following paragraphs.

84

85 The Pacific Stratus Sulfur Investigation, PSI-91 is the first cruise reported here. It took place in spring of
86 1991 in the eastern North Pacific off the coast of Washington state with the NOAA *R/V Discoverer*
87 leaving from Seattle, WA in mid-April and returning in early May. Measurements focused on the role of

88 DMS oxidation products in new particle production versus particle growth (Quinn et al., 1993; Covert et
89 al., 1992) and the seawater sulfur cycle (Bates et al., 1994).

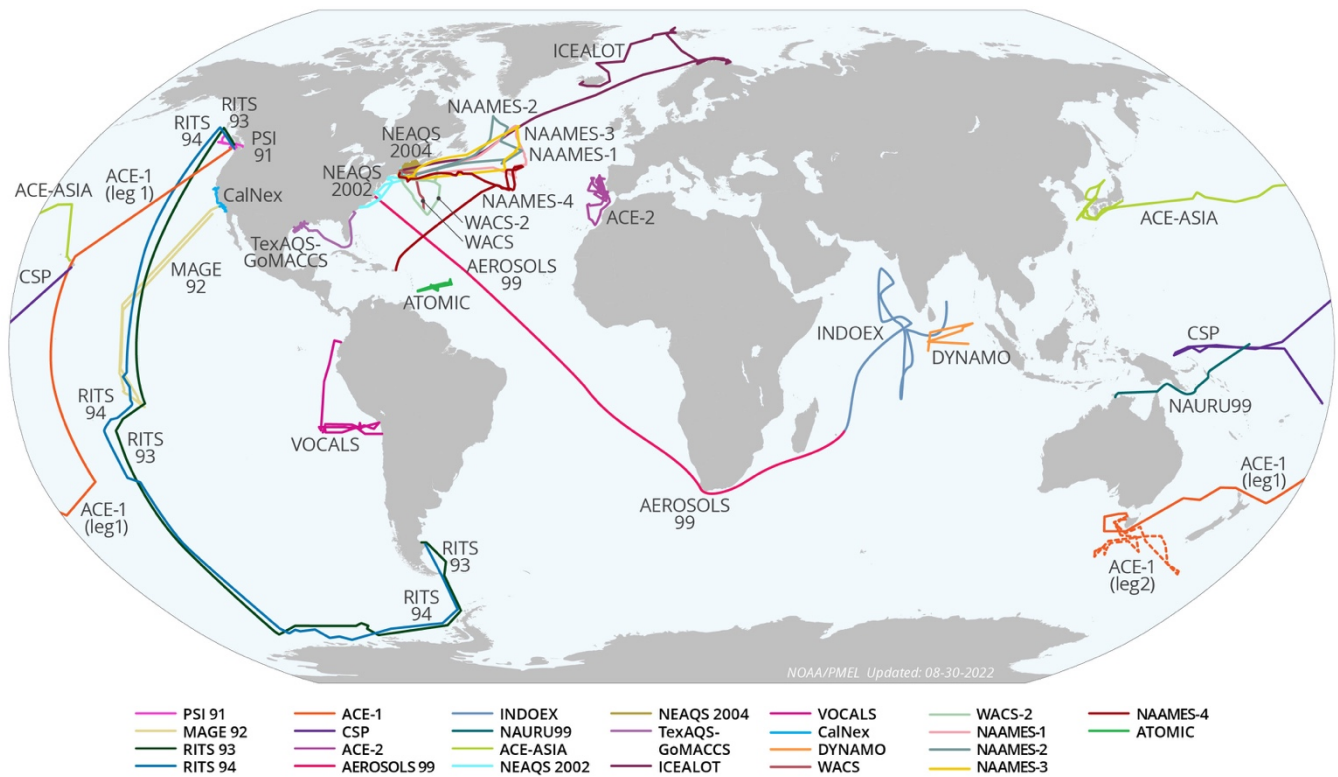
90

91 The Marine Aerosol and Gas Exchange cruise (MAGE92) took place in the tropical Pacific in 1992 with
92 the USC *R/V John Vickers* leaving from Los Angeles, CA in mid-February, transiting to Nuka Hiva in
93 the Marquesas Islands, and then returning to Los Angeles in late March. Similar to PSI-91, the goals of
94 MAGE92 were to assess the seawater sulfur cycle and processes controlling the atmospheric aerosol
95 particle number size distribution in the marine boundary layer (MBL) (Covert et al., 1996). In addition,
96 instrumentation was augmented to include an integrating nephelometer to measure the aerosol light
97 scattering coefficient at 550 nm (Charlson et al., 1967). The measurements were used to assess variability
98 in aerosol chemical, microphysical, and optical properties relevant to direct radiative forcing (Quinn et
99 al., 1995).

100

101 ***Figure 1. Cruise tracks for PMEL cruises between 1991 and 2020.***

102



103

104

105 The Radiatively Important Trace Species (RITS) cruises, RITS93 and RITS94, took place between March
 106 and May 1993 and November 1993 and January 1994, respectively. During RITS93, the NOAA *R/V*
 107 *Surveyor* went from Palmer Station, Antarctica to the Gulf of Alaska while RITS94 went in the opposite
 108 direction. These cruises extended the measurements made during MAGE92 to the central Pacific between
 109 55°N and 70°S (Quinn et al., 1996; Covert et al., 1996; Anderson et al., 1996).

110

111 In 1995, a series of Aerosol Characterization Experiments (ACE) was initiated under the auspices of the
 112 International Global Atmospheric Chemistry (IGAC) Project. The overall goal of ACE was to quantify
 113 the chemical and physical processes controlling the properties and evolution of aerosol particles relevant
 114 to radiative forcing and climate. Each experiment was multi-platform (research ships, aircraft, and ground
 115 stations) with international participation. The first Aerosol Characterization Experiment (ACE-1) took
 116 place in the Southern Ocean to target aerosol in a remote, minimally polluted marine atmosphere as a

117 reference for future experiments (Bates et al., 1998a). PMEL conducted measurements onboard the
118 NOAA *R/V Discoverer* during Leg 1 from Seattle, WA, USA to Hobart, Australia and then Leg 2 in the
119 Southern Ocean in and out of Hobart, Australia. ACE-1 extended earlier Pacific measurements to the
120 Southern Ocean and augmented the characterization of optical properties through the addition of a single
121 wavelength (550 nm) Particle Soot Absorption Photometer (PSAP) (Quinn et al., 1998b).

122

123 Subsequent ACEs were conducted downwind of continents to characterize changes in aerosol properties
124 with advection over the ocean. ACE-2 was conducted in June and July of 1997 over the sub-tropical
125 northeast Atlantic to characterize pollution and dust aerosol as it was advected from Europe and Africa
126 and mixed into the marine atmosphere (Raes et al., 2000). PMEL made measurements onboard the
127 Institute of Biology of the Southern Seas (IBSS) *R/V Professor Vodyanitskiy* leaving from and returning
128 to Lisbon, Portugal. Background marine, anthropogenic, and dust aerosol were encountered (Bates et al.,
129 2000). Instrumentation was unchanged from that of previous cruises.

130

131 The third experiment in the series was the Indian Ocean Experiment (INDOEX) which targeted the Indo-
132 Asian haze during the Northern Hemisphere dry monsoon as it was advected over the Indian Ocean
133 (Ramanathan et al., 2001). PMEL participated onboard the NOAA *R/V Ronald H. Brown* in a leg which
134 brought the ship from Norfolk, VA to Mauritius during January and February of 1999. This leg was named
135 AEROSOLS99. The second leg, officially INDOEX, took the ship from Mauritius northeast throughout
136 the South Atlantic and Indian Oceans and ended in the Maldives during February and March of 1999.
137 During both legs, marine background, anthropogenic, dust, and biomass burning aerosol were measured
138 (Quinn et al., 2001). Trace element concentrations able to identify and quantify dust were added to the
139 PMEL instrument payload for AEROSOLS99 and INDOEX.

140 ***Table 1. PMEL's cruises between 1991 and 2020 with start and stop dates, departure and arrival***
141 ***ports, ocean, and relevant references.***

142

	Dates		Ports		Ocean(s)	References
	Start	Stop	Departure	Arrival		
PSI-91 ^a	4/15/1991	5/1/1991	Seattle, WA, USA	Seattle, WA, USA	North Pacific (coastal Washington)	Covert et al. (1992); Quinn et al. (1993)

MAGE92 ^b	2/21/1992	3/25/1992	Los Angeles, CA, USA	Nuka Hiva, Marquesas Islands	Tropical Pacific	Quinn et al. (1995)
RITS93 ^c	3/20/1993	5/7/1993	Punta Arenas, Chile	Seattle, WA, USA	South and Tropical Pacific	Covert et al. (1996)
RITS94 ^d	11/20/1993	1/7/1994	Seattle, WA, USA	Punta Arenas, Chile	North and Tropical Pacific	Covert et al. (1996)
ACE-1 ^e Leg 1	10/12/1995	11/9/1995	Seattle, WA, USA	Hobart, Australia	Pacific	Bates et al. (1998a)
ACE-1 ^e Leg 2	11/15/1995	12/13/1995	Hobart, Australia	Hobart, Australia	Southern Ocean	Bates et al. (1998a)
CSP ^f	3/12/1996	4/13/1996	Pago Pago, American Samoa	Honolulu, HI, USA	Tropical Pacific	Post et al. (1997)
ACE-2 ^g	6/18/1997	7/24/1997	Lisbon, Portugal	Lisbon, Portugal	Northeast Atlantic	Raes et al. (2000)
AEROSOLS99	1/14/1999	2/8/1999	Norfolk, VA, USA	Cape Town, South Africa	Atlantic	Bates et al. (2001)
INDOEX ^h	2/22/1999	3/30/1999	Mauritius	Male, Maldives	South Atlantic and Indian	Ramanathan et al. (2001)
NAURU99 ⁱ	6/15/1999	7/19/1999	Darwin, Australia	Kwajalein, Marshall Islands	Tropical Pacific	Post et al. (2000)
ACE-Asia ^j	3/15/2001	4/20/2001	Honolulu, HI, USA	Yokosuka, Japan	Western Pacific	Bates et al. (2004); Huebert et al. (2003)
NEAQS 2002 ^k	7/12/2002	8/11/2002	Charleston, SC, USA	Charleston, SC, USA	Gulf of Maine, Atlantic Ocean	Bates et al. (2005)
NEAQS 2004 ^l	7/5/2004	8/12/2004	Portsmouth, NH, USA	Portsmouth, NH, USA	Gulf of Maine, Atlantic Ocean	Fehsenfeld et al. (2006)
TexAQS-GoMACCS ^m	7/27/2006	9/11/2006	Charleston, SC, USA	Galveston, TX, USA	Gulf of Mexico	Parrish et al. (2009); Bates et al. (2008)
ICEALOT ⁿ	3/19/2008	4/24/2008	Woods Hole, MA, USA	Reykjavik, Iceland	North Atlantic, Arctic Ocean	Quinn et al. (2017); Russell et al. (2010)
VOCALS ^o	10/13/2008	12/2/2008	Panama City, Panama	Arica, Chile	Tropical Pacific	Hawkins et al. (2010); Wood et al. (2011)
CalNex ^p	5/14/2010	6/8/2010	San Diego, CA, USA	San Francisco, CA, USA	California Coast	Ryerson et al. (2013); Bates et al. (2012)
DYNAMO ^q	9/29/2011	12/8/2011	Phuket, Thailand	Phuket, Thailand	Indian Ocean	Dewitt et al. (2013)
WACS ^r	8/19/2012	8/27/2012	Boston, MA, USA	St. George's, Bermuda	North Atlantic	Quinn et al. (2014); Keene et al. (2017)
WACS2 ^s	5/20/2014	6/5/2014	Woods Hole, MA, USA	Woods Hole, MA, USA	North Atlantic	Aller et al. (2017)
NAAMES1 ^t	11/6/2015	12/1/2015	Woods Hole, MA, USA	Woods Hole, MA, USA	North Atlantic	Quinn et al. (2019); Quinn et al. (2017); Behrenfeld et al. (2019)

NAAMES2 ^a	5/11/2016	6/5/2016	Woods Hole, MA, USA	Woods Hole, MA, USA	North Atlantic	Quinn et al. (2019); Quinn et al. (2017); Behrenfeld et al. (2019)
NAAMES3 ^b	8/30/2017	9/24/2017	Woods Hole, MA, USA	Woods Hole, MA, USA	North Atlantic	Quinn et al. (2019); Quinn et al. (2017); Behrenfeld et al. (2019)
NAAMES4 ^c	3/20/2018	4/13/2018	San Juan, Puerto Rico	Woods Hole, MA, USA	Tropical and North Atlantic	Quinn et al. (2019) Behrenfeld et al. (2019)
ATOMIC ^d	1/7/2020	2/13/2020	Bridgetown, Barbados	Bridgetown, Barbados	Tropical Atlantic	Quinn et al. (2021)

143

144 ^aPacific Stratus Sulfur Investigation 1991

145 ^bMarine Aerosol and Gas Exchange 1992

146 ^cRadiatively Important Trace Species 1993

147 ^dRadiatively Important Trace Species 1994

148 ^eAerosol Characterization Experiment-1 (<https://data.eol.ucar.edu/project/ACE-1>)

149 ^fCombined Sensor Program (<https://psl.noaa.gov/psd3/air-sea/csp/>)

150 ^gAerosol Characterization Experiment-2

151 ^hIndian Ocean Experiment (<http://www.indoex.ucsd.edu/index.html>)

152 ⁱ<https://psl.noaa.gov/psd3/air-sea/nauru99/>

153 ^jAerosol Characterization Experiment-Asia (https://www.eol.ucar.edu/field_projects/ace-asia)

154 ^kNew England Air Quality Study 2002 (<https://csl.noaa.gov/projects/neaqs/>)

155 ^lNew England Air Quality Study and International Consortium for Atmospheric Research on Transport and Transformation 2004 (<https://csl.noaa.gov/projects/icartt/>)

157 ^mTexas Air Quality Study/Gulf of Mexico Atmospheric Composition and Climate Study (<https://csl.noaa.gov/projects/2006/>)

158 ⁿInternational Chemistry Experiment in the Arctic Lower Troposphere

159 ^oVAMOS Ocean-Cloud-Atmosphere-Land Study (https://www.eol.ucar.edu/field_projects/vocals)

160 ^pCalifornia Research at the Nexus of Air Quality and Climate Change (<https://csl.noaa.gov/projects/calnex/>)

161 ^qDynamics of the Madden-Julian Oscillation (https://www.eol.ucar.edu/field_projects/dynamo)

162 ^rWestern Atlantic Climate Study 2012

163 ^sWestern Atlantic Climate Study 2014 (https://saga.pmel.noaa.gov/field_WACS2)

164 ^tThe North Atlantic Aerosols and Marine Ecosystem Study-1 (<https://science.larc.nasa.gov/NAAMES/>)

165 ^uAtlantic Tradewind Ocean-Atmosphere Mesoscale Interaction Campaign (<https://psl.noaa.gov/atomic/>)

166

167

168 ACE-Asia, the fourth and final of the ACEs, was conducted in March through May of 2001 downwind of
169 eastern Asia to target seasonal outbreaks of Asian dust associated with frontal systems moving to the east
170 through dust-producing regions (Huebert et al., 2003). PMEL sampled onboard the NOAA *R/V Ronald*
171 *H. Brown* from mid-March to mid-April in 2001 as the ship transited from Honolulu, HI to the western
172 Pacific and then spent time east of Japan and in the Sea of Japan. Between Honolulu and 2,000 mile east
173 of Japan, marine air minimally impacted by continental emissions was sampled. West onward from that

174 point, air masses heavily influenced by Asian emissions were sampled (Bates et al., 2004). Measurements
175 of organic carbon (OC) and elemental carbon (EC) were added to the instrument payload for ACE-Asia.
176

177 During the ACE years, PMEL participated in two other cruises, the Combined Sensor Program (CSP) in
178 March and April 1996 and NAURU99 in June and July of 1999. CSP took place in the central and tropical
179 western Pacific with the NOAA *R/V Discoverer* leaving from Pago Pago, American Samoa in mid-March
180 and arriving in Honolulu, HI in mid-April. The overarching goal of CSP was to better understand
181 relationships between atmospheric and oceanic variables that affect radiative balance, including aerosol
182 particles (Post et al., 1997). NAURU99 took place onboard the NOAA *R/V Ronald H. Brown* in the
183 southwestern Pacific in the vicinity of Nauru Island in Papua New Guinea. NAURU99 had similar
184 scientific goals as CSP and, in addition, was conducted to assess how representative measurements made
185 on the islands of Nauru and Manus were of the surrounding ocean (Post et al., 2000). The ship left Darwin,
186 Australia in mid-June and arrived in Kwajalein in the Marshall Islands in mid-July.

187

188 In 2002, a series of air quality and climate field campaigns was initiated by NOAA with other agency and
189 academic partners. These campaigns were designed to determine the atmospheric processes that control
190 the production and distribution of air pollutants that impact air quality and climate in and downwind of
191 several U.S. regions. These campaigns involved, to varying degrees, a combination of shipboard, aircraft,
192 and ground-based measurements. The New England Air Quality Study in 2002 (NEAQS 2002) targeted
193 factors controlling air quality in New England with measurements at a network of ground stations and a
194 ship (Bates et al., 2005). The NOAA *R/V Ronald H. Brown* departed Charleston, SC in mid-July 2002
195 and transited northeast up the coast to New York City, Boston, and Acadia National Park in Maine. The
196 ship returned to Charleston in mid-August 2002.

197

198 A second NEAQS in 2004 (NEAQS 2004) was conducted in conjunction with the joint North American
199 and European International Consortium for Atmospheric Research on Transport and Transformation
200 (ICARTT). The focus was on emissions from North America and their chemical transformations and
201 removal during transport over the North Atlantic (Fehsenfeld et al., 2006). The NOAA *R/V Ronald H.*

202 *Brown* left Portsmouth, NH in early July, made several transits along the coasts of Massachusetts, New
203 Hampshire, and Maine, and across the Gulf of Maine toward Nova Scotia (Quinn et al., 2006). A
204 Quadruple Aerosol Mass Spectrometer (Q-AMS) (Jayne et al., 2000) was added to the PMEL instrument
205 payload for the measurement of nonrefractory (NR) species where NR refers to chemical components
206 that vaporize (< 5 sec) at the vaporizer temperature of ~550°C.

207

208 The next in the series of Air Quality – Climate cruises was the Texas Air Quality – Gulf of Mexico
209 Atmospheric Composition and Climate Study (TexAQS/GoMACCS) between July and September in
210 2006. The goal was to assess the factors that control the formation and transport of air pollutants along
211 the Gulf Coast of south eastern Texas and the impact the resulting species have on the radiative forcing
212 of climate regionally and globally (Parrish et al., 2009). The NOAA *R/V Ronald H. Brown* left Charleston,
213 SC at the end of July, headed south along the coast of Florida, transited across the Gulf of Mexico, and
214 spent several weeks along the coast of Texas including in the Houston Ship Channel (Bates et al., 2008).
215 The cruise ended mid-September in Galveston, TX. Measurements of the relative humidity dependence
216 of light scattering and cloud condensation nuclei (CCN) concentrations were added to the existing PMEL
217 instrument payload.

218

219 The final Air Quality – Climate field campaign was the 2010 California Research at the Nexus of Air
220 Quality and Climate Change (CalNex) study. An emphasis was put on issues that are simultaneously
221 relevant to both air pollution and climate including emission inventories, atmospheric transport and
222 dispersion, atmospheric processing, and aerosol direct and indirect radiative effects (Ryerson et al., 2013).
223 The Woods Hole Oceanographic Institution (WHOI) *R/V Atlantis* left from San Diego, CA in mid-May
224 2020, transited northward up the coast of California with incursions into the Ports of Los Angeles, Long
225 Beach, San Francisco, and Oakland, and a trip up the Sacramento River (Bates et al., 2012).

226

227 In between TexAQS-GoMACCS and CalNex, PMEL participated in two other cruises. The International
228 Chemistry Experiment in the Arctic Lower Troposphere (ICEALOT) took place as part of the 2008
229 International Polar Year (Russell et al., 2010). The focus was on the sources, transport, and climate impact

230 of anthropogenic aerosol and gas phase species in an ice-free region of the Arctic. The WHOI *R/V Knorr*
231 left Woods Hole, MA mid-March, transited across the North Atlantic to the coast of Norway, then
232 northwest to Svalbard, and southwest to Reykjavik, Iceland where the cruise concluded at the end of
233 April.

234

235 The VAMOS Ocean-Cloud-Atmosphere-Land Study Regional Experiment (VOCALS), where VAMOS
236 stands for Variability of the American Monsoon Systems, took place in October and November of 2008.
237 VOCALS focused on assessing links between aerosols, clouds and precipitation and their impacts on
238 marine stratocumulus radiative properties and couplings between the upper ocean and lower atmosphere
239 (Wood et al., 2011). The NOAA *R/V Ronald H. Brown* left Panama City, Panama in mid-October,
240 conducted several transits in the vicinity of 20°S from the coast to 85°W, and ended the cruise in Arica,
241 Chile at the beginning of December (Hawkins et al., 2010).

242

243 DYNAMO, the Dynamics of the Madden-Julian Oscillation (MJO) field campaign was conducted to
244 collect *in situ* observations to advance our understanding of MJO initiation processes and to improve
245 MJO prediction (Yoneyama et al., 2013). PMEL's research focused on the effect of MJO-associated
246 convection anomalies on aerosols in the marine boundary layer (Dewitt et al., 2013). The Scripps
247 Institution of Oceanography *R/V Roger Revelle* left Phuket, Thailand at the end of September 2011 and
248 transited to the vicinity of 0.1°N and 80.5°E where it was stationed for most of the experiment. The ship
249 returned to Phuket on December 8.

250

251 Between 2012 and 2018, PMEL participated in a series of cruises to investigate the impacts of marine
252 ecosystems on primary sea spray aerosol (SSA) and its cloud-nucleating properties. During each of these
253 cruises a portion of the time was spent generating and sampling nascent primary SSA with Sea Sweep
254 (Bates et al., 2012). The Sea Sweep data are available in the referenced data sets for WACS, WACS-2,
255 and all four NAAMES cruises. These data are not discussed further since the emphasis here is on ambient
256 aerosol. Data from the ambient atmospheric marine aerosol that was sampled when Sea Sweep was not
257 in use are discussed here. The first Western Atlantic Climate Study (WACS) took place in 2012 and

258 focused on the high-chlorophyll, biologically productive region of Georges Bank off the coast of Cape
259 Cod and the low-chlorophyll, oligotrophic Sargasso Sea (Quinn et al., 2014; Kawamura et al., 2017). The
260 NOAA *R/V Ronald H. Brown* left Boston, MA in mid-August, spent time at the high- and low-chlorophyll
261 stations, and arrived at St. George's Bermuda at the end of August.

262

263 The second WACS (WACS2) took place in 2014. The WHOI *R/V Knorr* left Woods Hole, MA in mid-
264 May, went east to 60°W and south to 33°S stopping for stations at a range of low to high biologically
265 productive surface seawater. Atmospheric sampling took place between stations. The ship arrived back
266 in Woods Hole in the beginning of June (Aller et al., 2017).

267

268 PMEL participated in the NASA sponsored North Atlantic Aerosols and Marine Ecosystems Study
269 (NAAMES), a series of field campaigns conducted to assess the seasonal impact of the western subarctic
270 North Atlantic phytoplankton bloom on aerosols and clouds (Behrenfeld et al., 2019). Four cruises,
271 onboard the WHOI *R/V Atlantis*, took place between November 2015 and April 2018, with each cruise
272 targeting specific seasonal phases of the annual plankton cycle (Quinn et al., 2019). The general cruise
273 track included a transit from Woods Hole, MA to 40°N and 40°W, a northward transit with several stations
274 to 55°N across a range of stages in each plankton seasonal cycle, followed by a return to Woods Hole.
275 The exception was NAAMES-4, which left from San Juan, Puerto Rico and ended in Woods Hole. In
276 seasonal but not chronological order, NAAMES-1 took place in November 2015 targeting the initiation
277 of the phytoplankton blooming phase, NAAMES-4 in March and April 2018 targeting the accumulation
278 phase, NAAMES-2 in May and June targeting the bloom climax, and NAAMES-3 in September 2017
279 targeting the declining phase of the bloom. To accommodate Sea Sweep sampling, atmospheric sampling
280 of trace elements, NR chemical species, and total aerosol mass was not conducted during any of the
281 NAAMES cruises.

282

283 The final cruise in the global data set to date is the Atlantic Tradewind Ocean-Atmosphere Mesoscale
284 Interaction Campaign (ATOMIC) which took place in the tropical North Atlantic east of Barbados in
285 early 2020 (Stevens et al., 2021). The NOAA *R/V Ronald H. Brown* left Bridgetown, Barbados in early

286 January and spent time between Barbados and the Northwest Tropical Atlantic Station (NTAS) buoy 500
287 nm to the northeast to gather information on shallow atmospheric convection, the effects of aerosols and
288 clouds on the ocean surface energy budget, and mesoscale oceanic processes (Quinn et al., 2022).
289 Measurements of trace element and total aerosol mass concentrations were reinstated for ATOMIC but
290 concentrations of NR chemical species were not.

291

292 **3. Methods**

293

294 Sampling methods evolved between 1991 and 2020 as the number of parameters to be measured increased
295 and the technical capabilities of instrumentation improved. In addition, instruments were added or
296 removed from the PMEL payload depending on the goals of each cruise. Instrumentation and its evolution
297 are described in detail below including the sampling inlet and methods for the measurement of aerosol
298 microphysical, chemical, optical, and cloud-nucleating properties. In addition, measurement methods of
299 gas phase species and surface seawater properties are provided. Parameters measured during each cruise
300 are listed in Table 2 (aerosol microphysical and cloud-nucleating), Table 3 (aerosol chemical
301 composition), Table 4 (aerosol optical), and Table 5 (gas phase and seawater species).

302

303 For all cruises, instrumentation was housed in one or more 8 ft (2.44 m) tall shipping container(s) outfitted
304 with power, air conditioning, and, in some cases, water. Unistrut was installed on inside walls for the
305 securing of instrument racks, drawers, shelves, etc. A railing surrounding the sampling inlet was installed
306 on the roof of the container for mounting of meteorological and other sensors.

307

308 **3.1. Aerosol sampling inlet**

309

310 For all cruises, an aerosol sampling mast was mounted on top of an 8 ft (2.44 m) tall shipping container
311 converted to a laboratory as described above. Diagrams of the sampling inlet and connections to
312 instrumentation are shown in Figure 2. Schematics for all parts of the sampling inlet can be found at
313 <https://www.pmel.noaa.gov/acg/gallery/aerosol-sampling-inlet-schematics>. The container was mounted

314 as far forward of the ship's stack as possible to minimize contamination. To maintain nominally isokinetic
315 flow and minimize the loss of supermicron particles, the inlet at the top of the mast was rotated into the
316 relative wind first manually (PSI-91 to NAURU-99) and then automatically under computer control (ACE
317 Asia through ATOMIC). The mast angle was recorded for post-cruise data analysis. Air entered the inlet
318 through a 5 cm diameter hole, passed through an expansion cone, and then into the 20 cm diameter
319 sampling mast. The flow through the mast was $1 \text{ m}^3 \text{ min}^{-1}$. Individual 1.9 cm diameter stainless steel tubes
320 extended into the base of the mast. These were connected to the various aerosol instruments in the
321 laboratory container directly below the mast with carbon-embedded conductive tubing to prevent the loss
322 of particles through static charging. Sampling of organics was added to the PMEL payload for ACE-Asia.
323 Stainless steel tubing was added for the connections between the aerosol inlet and the instruments and
324 impactors sampling for organic components.

325

326 During the initial cruise reported here, PSI-91, sample air from the mast was not conditioned, i.e., heated
327 to control RH. Instead, aerosol was sampled at ambient RH ($75 \pm 9\%$) although all CPCs (Condensation
328 Particle Counters) had diffusion dryers upstream to reduce the RH of the sample air to less than 30%.
329 Aerosol microphysical properties were measured continuously with periods of contamination, calibration,
330 and downtime removed from the final data set. To avoid contamination by the ship's stack, samples for
331 chemical analysis were collected only when the particle number concentration measured at the top of the
332 mast was less than 1000 cm^{-3} , the relative wind speed was greater than 3 m s^{-1} , and the relative wind
333 direction was forward of the ship's beam ($\pm 90^\circ$). This approach was employed during all cruises although
334 the particle number concentration and relative wind speed and direction limits were varied depending on
335 conditions.

336

337 After PSI-91, the last 1.5 m of the inlet were heated to establish a low reference relative humidity. Heating
338 allows for constant instrumental size segregation in spite of variations in ambient RH and results in
339 measurements of aerosol chemical, microphysical, and optical properties that are directly comparable.
340 During MAGE 92, RITS 93, RITS 94, and ACE-1, sample air was heated above ambient temperatures to
341 reach an RH of $< 25\%$. The target RH for the sample air was increased to 55 to 60% for ACE-2 and

342 following cruises because it is above the efflorescence humidity of most aerosol components and
343 component mixtures (Carrico et al., 2003), which reduces particle bounce in impactors and simplifies
344 thermodynamic equilibrium calculations of particle density and refractive index. There are a few
345 exceptions to the target RH of 55 to 60%. The cold Arctic air temperatures during ICEALOT and the
346 higher latitude portions of the NAAMES cruises made it difficult to obtain that RH. Instead, the aerosol
347 was sampled at less than 25% RH during those conditions.

348

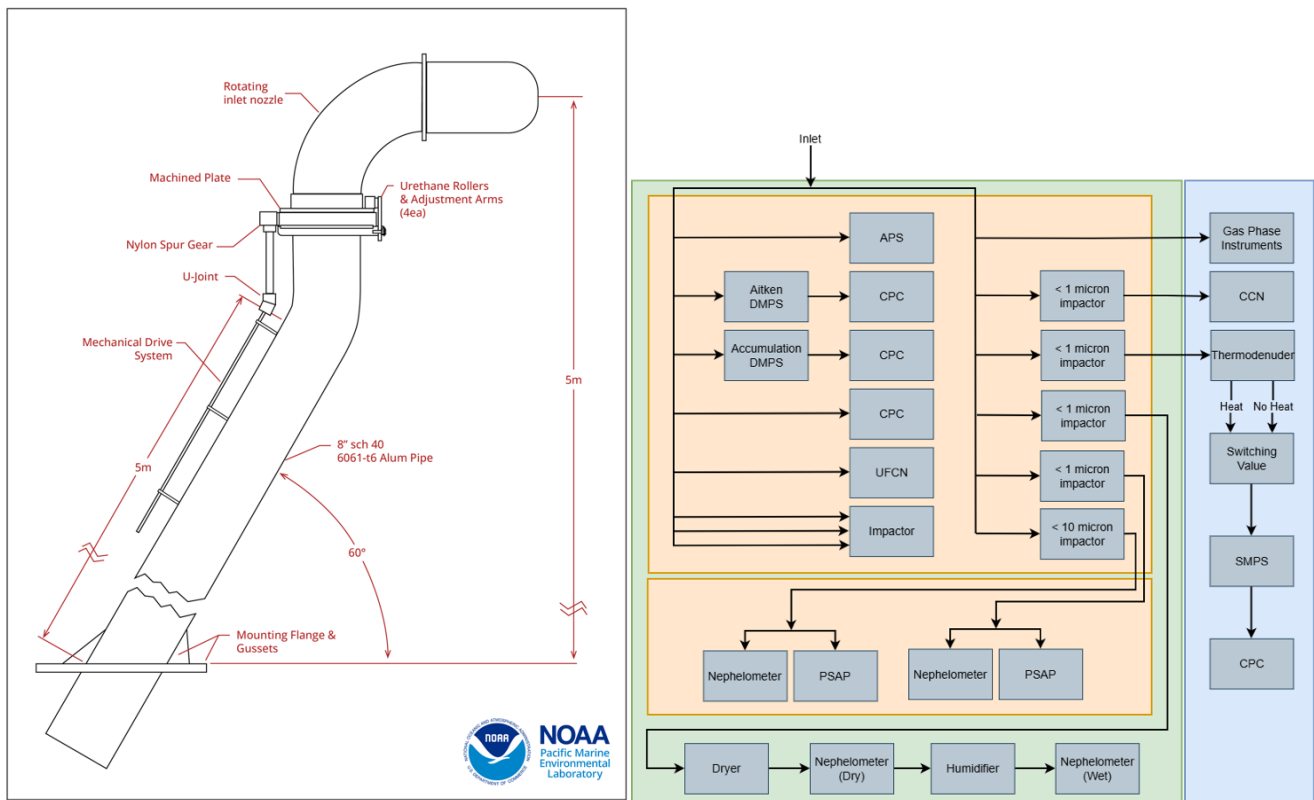
349 After RITS94 and before ACE-1, a temperature-controlled box was installed at the base of the sampling
350 mast (Figure 2b and c). The box was heated above ambient temperatures to reduce cooling and
351 condensation in sampling lines in the air-conditioned laboratory container and to maintain a uniform RH
352 of the sampled air. Instrumental RH for the particle sizing systems is listed in Table 2.

353

354 The transmission efficiency of particles through the mast as a function of size was characterized after
355 INDOEX in the Kirsten Wind Tunnel at the University of Washington (Bates et al., 2002). The Kirsten
356 Wind Tunnel is a subsonic, closed circuit, double return wind tunnel. The mast was mounted under the
357 wind tunnel with the rotatable cone on top extending into the test section of the tunnel. Two sets of
358 propellers moved air through the test section at speeds of 7 to 20 m sec⁻¹. Aerosol particles were generated
359 from a 10% polyethylene glycol solution (PEG-400 molecular weight mixed in distilled water) using a
360 pressurized tank and spray nozzle downwind of the mast. Aerosol size distributions were measured from
361 0.56 to 14 μm using Aerodynamic Particle Sizers (APS 3320, TSI, St. Paul, MN). Larger particle sizes
362 were the focus of these tests as comparisons of total particle number concentration during ACE-1 found
363 agreement within ~ 20% of the NCAR C-130 airplane and ground stations. The aerosol generator was

364

365 ***Figure 2. Shown are schematics of the aerosol sampling inlet (left) and a flow chart indicating the flow***
366 ***of sample air from the inlet to the instrumentation (right). This flow chart depicts the maximum***
367 ***number of instruments deployed. Green represents the van the inlet is mounted on, orange represents***
368 ***the temperature controlled box at the base of the inlet, and blue represents the van next door housing***
369 ***additional real time instruments.***



370

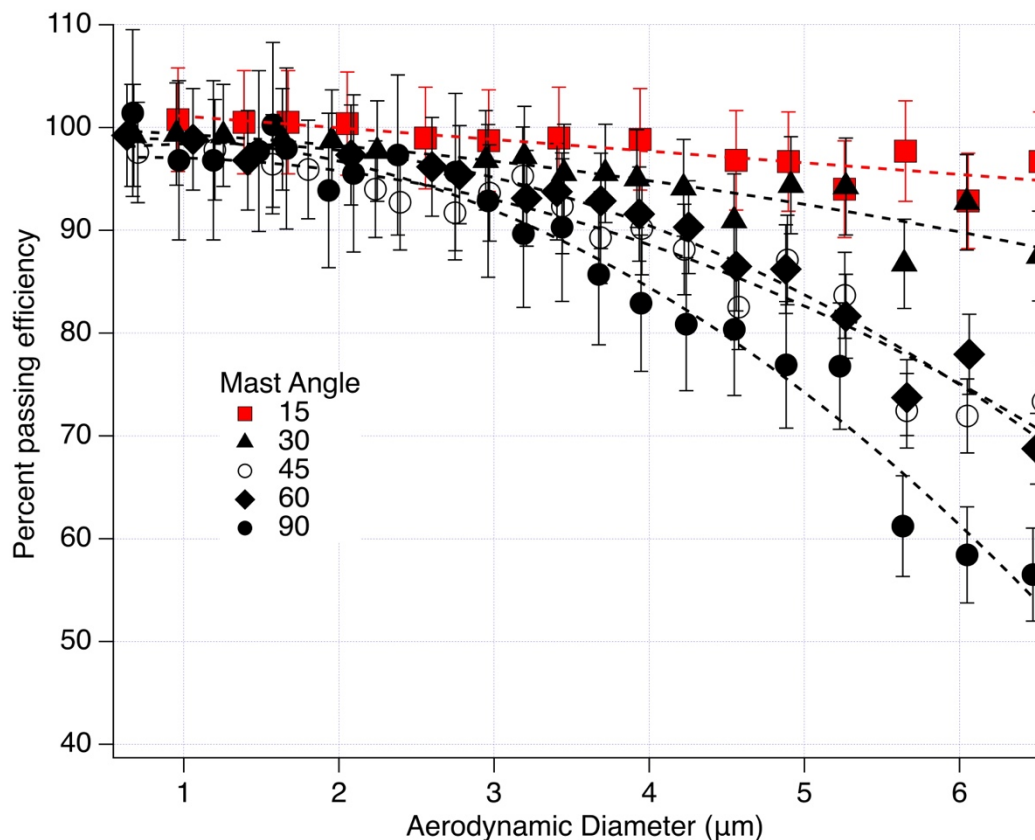
371

372 operated for 1 min every 5 min to maintain a steady concentration of ~ 500 particles per cm^3 . Tests were
 373 conducted at different angles (0 to 90°) between the wind vector and the mast inlet cone axis, different
 374 wind speeds (7 to 20 m sec^{-1}), and different air flows down the mast (30 to 1200 l min^{-1}). The only
 375 parameter that was found to affect the transmission efficiency was the angle between the wind and the
 376 mast inlet cone. The transmission efficiency for particles with diameters less than $6.5 \mu\text{m}$ was determined
 377 to be greater than 95% when the inlet was kept to within 15° of the wind direction (Figure 3). At a 90°
 378 angle, the inlet transmitted about 60% of the particles in the $6 \mu\text{m}$ size bin. Data collected in bins greater
 379 than $6.5 \mu\text{m}$ were within the instrument noise level due to Poisson counting statistics.

380

381

382 *Figure 3. Percent transmission efficiency of the mast at different angles between the inlet nozzle and*
 383 *the wind direction. The vertical bars indicate one standard deviation of the mean efficiency in each*
 384 *size bin. The curves are a second-order polynomial fit through the data at each angle. From Bates et*
 385 *al. (2002).*



386
 387
 388

389 3.2. Aerosol microphysical properties

390

391 Total particle number concentration was measured on all cruises. After the first cruise, PSI-91, number
 392 size distributions were measured on all cruises. Measurements of cloud condensation nuclei (CCN)
 393 concentrations were first added in 2006 for TexAQS. Details of the measurements are outlined below.
 394 Table 2 indicates the measurement methods used on each cruise and, in the case of number size
 395 distributions, the instrumental RH.

396

397 **3.2.1. Particle number concentrations**

398 As indicated in Table 2, during the first several cruises (PSI-91, MAGE92, RITS93, RITS94), total
399 particle number concentrations for D_p greater than 3 and 12 nm were measured with TSI 3025 and 3760
400 CPCs, respectively. The ultrafine particle number concentration was then defined as the difference
401 between the number concentration measured with the 3025 and 3760 CPCs. For these initial cruises and
402 all subsequent ones, diffusion driers (Permapure Inc.) were placed upstream of the CPCs to minimize
403 particle diameter changes due to hygroscopic growth to less than 5% (Swietlicki et al., 2008). The use of
404 a diffusion drier also helped prevent the uptake of water in the CPC condenser that results when sampling
405 in the humid marine atmosphere. Beginning with ACE-2 in 1997 and continuing through ATOMIC in
406 2020, particle number concentrations for $D_p > 12$ nm were measured with a TSI 3010 CPC. Starting in
407 2008 for VOCALS, a water-based TSI 3785 CPC was added to also measure the concentrations of
408 particles with diameters greater than 3 nm.

409

410 **3.2.2. Particle number size distributions**

411 For MAGE92, RITS93, and RITS94, particle number size distributions from 0.02 to 0.6 μm were
412 measured with a TSI 3071 Differential Mobility Analyzer (DMA) (Quinn et al., 1998b) with the number
413 concentration in each bin measured with a TSI 3760 CPC. The resulting number mobility distributions
414 were inverted to a number size distribution by using the manufacturer-provided algorithm (Keady et al.,
415 1983) and assuming that a Fuchs-Boltzman equilibrium charge distribution resulted from a Kr^{85} charge
416 neutralizer (TSI model 3077) on the inlet of the DMA. The number concentration was corrected for the
417 counting efficiency of the CPC (Zang et al., 1991) and diffusion losses in the DMA (Reineking et al.,
418 1986). The sample air passed through a diffusion drier to reduce the RH to less than 25%.

419

420 A Vienna short column Ultrafine DMPS (UDMPS) coupled to a TSI 3025 CPC was added for ACE-1
421 and all subsequent cruises to extend the size distribution measurements to the 0.005 to 0.02 μm size range.
422 For both ACE-1 and CSP, the UDMPS and the TSI 3071 DMA were located outside of the temperature-
423 controlled box. Sheath air for both resulted in a measurement RH of less than 25% RH. As for the earlier

424 cruises, the mobility distributions were inverted to number size distributions by assuming that a Fuchs-
425 Boltzman charge distribution resulted from the Kr⁸⁵ charge neutralizers on the inlet of the DMAs. The
426 data were corrected for diffusional losses (Covert et al., 1997) and size dependent counting efficiencies
427 (Wiedensohler et al., 1997) based on pre-ACE-1 intercalibration exercises. In addition, an APS (TSI
428 3300) was added for ACE-1 and all subsequent cruises to measure the number size distribution between
429 0.6 and 9.6 μm . APS diameters measured at $\sim 40\%$ RH were converted to geometric diameters by dividing
430 by the square root of the particle density for sea salt (1.9 g cm^{-3}) and dried to 10% RH assuming a sea salt
431 growth factor of 1.5 between 10 and 40% RH (Berg et al., 1998).

432

433 For ACE-2 and all subsequent cruises, the UDMPS and TSI DMA were put into the temperature-
434 controlled box to maintain an instrumental RH of greater than 45% (see Table 2). The APS was also
435 transferred to the temperature-controlled box where it measured at an RH of approximately 40%.

436

437 For AEROSOLS99 and all subsequent cruises, a Vienna medium column DMPS was used to measure
438 particles in the 0.02 – 0.9 μm size range instead of the TSI 3071 DMA. In addition, the APS model 3300
439 was replaced with an APS model 3320. Duplicate Vienna medium column DMPSs were deployed for
440 AEROSOLS99 and INDOEX. One measured at 10% RH outside of the temperature-controlled box and
441 the other measured at 55% RH inside the box.

442

443 Although the APS was located in the temperature-controlled box and its inlet was maintained at 55% RH,
444 internal heating of the sample flow by its sheath flow and waste heat likely reduced the measurement RH
445 (Bates et al., 2004). For ACE-Asia and all subsequent cruises, the APS sheath flow was routed outside of
446 the instrument to equilibrate with the air temperature in the temperature-controlled box and then
447 reintroduced to the sheath and acceleration nozzle to lower the temperature and increase the measurement
448 RH. Also starting with ACE-Asia, densities and the associated water masses at the instrumental RH were
449 calculated with a thermodynamic equilibrium model (AeRho) using the measured inorganic ion
450 composition (Quinn et al., 1998a). These calculated densities were used to convert the APS data from
451 aerodynamic to geometric diameters for merging with the DMPS data. Due to the atmospheric dust that

452 was sampled during ACE Asia, the APS data were corrected for ultra-Stokesian conditions in the
453 instrument jet and nonspherical shape (Wang et al., 1987; Wang et al., 2002).

454

455 **3.2.3. Cloud condensation nuclei concentrations**

456 A CCN counter (DMT CCN-100) was added for TexAQS and several later cruises (CalNex, NAAMES-
457 1, NAAMES-2, NAAMES-3, NAAMES-4, and ATOMIC) (see Table 2). A CCN counter was onboard
458 during WACS and WACS2 but it sampled nascent SSA with Sea Sweep for the majority of the time.
459 CCN concentrations were measured at supersaturations between 0.2 and 1.0%. Details of the CCN counter
460 can be found in Roberts et al. (2005). A multijet cascade impactor (Berner et al., 1979) with a 50%
461 aerodynamic cut-off diameter of 1.1 μm was upstream of the CCN counter. More details about the CCN
462 measurements can be found in Quinn et al. (2008).

463

464 **3.3. Aerosol chemical composition**

465 The chemical species quantified along with sample collection and analysis methods are listed for each
466 cruise in Table 3 and described below. Starting with PSI-91, size segregated aerosol was collected with a
467 varying combination of two-, three-, and seven-stage multijet cascade impactors (Berner et al., 1979). All
468 impactors, except those used for the analysis of organic carbon, had a grease cup at the inlet of the
469 impactor that was coated with silicone grease to prevent the bounce of large particles onto the downstream
470 stages. Two stage impactors had 50% aerodynamic cut-off diameters, $D_{\text{aero},50}$, of 1.1 and 10 μm ; three
471 stage impactors had $D_{\text{aero},50}$, of 0.18, 1.1, and 10 μm ; and seven stage impactors had $D_{\text{aero},50}$, of 0.18, 0.31,
472 0.55, 1.1, 2.0, 4.1, and 10 μm . To attain these size cuts, air flow through all impactors was maintained at
473 30 lpm. Flow through the impactors was computer-controlled so that aerosol was only collected when the
474 relative wind speed and direction along with measured particle number concentration indicated there was
475 no contamination from the ship's stack. Chemical analysis of the substrates included ion chromatography
476 (inorganic ions), thermal/optical analysis (OC and EC), energy dispersive X-ray fluorescence (trace
477 elements), and gravimetric mass (total aerosol mass). The substrates used in the impactors depended on
478 the chemical species analyzed and are described below. Blank levels were determined by placing a
479 substrate in the impactor with no air pulled through it. Blank concentrations were subtracted from sample

480 **Table 2. Microphysical and cloud-nucleating properties measured on each cruise and the**
 481 **instrumentation used.**

Measured parameter and method	Cruise	482
UFCN^a, D_p > 3 nm TSI 3025 CPC ^b	PSI-91, MAGE92, RITS93, RITS94, ACE-1, CSP, ACE-2, AEROSOLS99, INDOEX, NAURU99, ACE-Asia, NEAQS 2002, NEAQS 2004, TexAQS, ICEALOT	
UFCN, D_p > 3 nm TSI 3785 CPC	VOCALS, CalNex, DYNAMO, WACS, WACS-2, NAAMES-1, NAAMES-2, NAAMES-3, NAAMES-4, ATOMIC	
CN^c > 12 nm TSI 3760 CPC	PSI-91, MAGE92, RITS93, RITS94	
CN > 12 nm TSI 3010 CPC	ACE-2, AEROSOLS99, INDOEX, NAURU99, ACE-Asia, NEAQS 2002, NEAQS 2004, TexAQS, ICEALOT, VOCALS, CalNex, DYNAMO, WACS, WACS-2, NAAMES-1, NAAMES-2, NAAMES-3, NAAMES-4, ATOMIC	
Number size distribution TSI 3071 DMA ^d , 0.02 – 0.6 μm	MAGE92, RITS93, RITS94 (< 25% RH)	
Number size distribution Vienna short column UDMPS ^e , 0.005 – 0.02 μm TSI 3071 DMA, 0.02 – 0.6 μm TSI 3300 APS ^f , 0.6 – 9.6 μm	ACE-1, CSP (< 25% RH); ACE-2 (45% RH)	
Number size distribution Vienna short column UDMPS, 0.005 – 0.02 μm Vienna medium column DMPS ^g , 0.02 – 0.9 μm TSI 3320 APS, 0.6 – 9.6 μm	AEROSOLS99, INDOEX (10 and 55% RH); NAURU99, ACE-Asia, NEAQS 2002, NEAQS 2004 (55% RH); TexAQS, VOCALS, CalNex, DYNAMO, CalNex, WACS, WACS-2, ATOMIC (60% RH); ICEALOT (< 25% RH); NAAMES-1, NAAMES-2, NAAMES-3, NAAMES-4 (<30 and 60% RH)	
CCN^h DMT CCN-100	TexAQS, ICEALOT, CalNex, NAAMES-1, NAAMES-2, NAAMES-3, NAAMES-4, ATOMIC	

483 ^aUltrafine Condensation Nuclei

484 ^bCondensation Particle Counter

485 ^cCondensation Nuclei

486 ^dDifferential Mobility Analyzer

487 ^eUltrafine Differential Mobility Particle Sizer

488 ^fAerodynamic Particle Sizer

489 ^gDifferential Mobility Particle Sizer

490 ^hCloud Condensation Nuclei

491

492

493

494 concentrations.

495

496 Additional chemical analyses were performed with a particle-into-liquid-sampler (PILS) followed by ion
497 chromatography and water soluble organic carbon (WSOC) analysis and an aerosol mass spectrometer
498 (AMS) for non-refractory (NR) analytes. Details are provided below.

499

500 **3.3.1. Inorganic ions**

501 A seven stage multi-jet cascade impactor was used on all cruises to collect size segregated samples for
502 ion chromatography analysis. The ions quantified were Na^+ , NH_4^+ , K^+ , Ca^{2+} , Mg^{2+} , Cl^- , NO_3^- , SO_4^{2-} , and
503 methane sulfonate or MSA^- . A Millipore Fluoropore filter (1.0 μm pore size) was used for the final,
504 smallest size range stage. The Millipore filter has a collection efficiency of 99% or greater for particles
505 with diameters larger than 0.035 μm (Liu et al., 1976). Tedlar films were used for the six largest stages.
506 The films were cleaned in an ultrasonic bath in 10% H_2O_2 for 30 min, rinsed 6 times in distilled, deionized
507 water, and then dried in an NH_3 - and SO_2 -free glove box. Material collected on the filters and films was
508 extracted by wetting with 1 mL of methanol and then adding 5 mL of distilled deionized water and
509 sonicating for 30 min. Samples were handled in a glove box that was purged with air that had passed
510 through a scrubber containing potassium carbonate, citric acid, and activated charcoal to remove SO_2 ,
511 NH_3 , and volatile organics, respectively. Sampling times varied between ~12 and 36 hrs and were based
512 on the amount of aerosol present.

513

514 For the first few cruises (MAGE92, RITS93, RITS94), higher time resolution (< 12 hrs) submicron
515 aerosol samples were collected using a filter holder downstream of a cyclone with a $D_{\text{aero},50}$ of 1 μm .
516 Starting with ACE-1, a 2-stage impactor was used for higher time resolution sampling of sub- and
517 supermicron aerosol for ion chromatography analysis. Substrates, sample handling, and blank
518 determinations were the same as discussed above.

519

520 A Particle-Into-Liquid-Sampler (PILS) coupled to an ion chromatograph was used to sample submicron
521 inorganic ions during NEAQS 2002, NEAQS 2004, and TexAQS at a higher time resolution (15 min)

522 than any of the impactors (Bates et al., 2008). The common aerosol inlet was used to deliver aerosol to a
523 PILS at 55% RH. An impactor with a $D_{aero,50}$ of 1.1 μm was upstream of the PILS. Flow through the
524 impactor was 30 slpm with 15 slpm through the PILS and 15 slpm through a bypass line. Two annular,
525 glass denuders (URG) were in series downstream of the impactor and upstream of the PILS. One was
526 coated with sodium carbonate for the removal of gas phase acids and the other was coated with citric acid
527 to remove gas phase bases. Two Kloehn syringe pumps were used to deliver a solution of LiF to the top
528 of the PILS impactor to correct for dilution of the sample within the PILS. Two additional pumps
529 delivered sample from the PILS simultaneously to a cation and an anion IC. More information about the
530 PILS can be found in (Weber et al., 2001). Between every 45 min to 2 hrs, sample air was passed through
531 a HEPA filter for 15 min to remove particles and determine the measurement blank. This blank was
532 subtracted from the sample concentrations.

533

534 For both the impactor and the PILS data, non-sea salt (nss) SO_4^- concentrations were calculated from Na^+
535 concentrations and the ratio of sulfate to sodium in seawater. Sea salt concentrations were calculated from
536

$$537 \quad \text{Sea salt } (\mu\text{g m}^{-3}) = \text{Cl}^- (\mu\text{g m}^{-3}) + \text{Na}^+ (\mu\text{g m}^{-3}) \times 1.47 \quad (1)$$

538

539 where 1.47 is the seawater ratio of $(\text{Na}^+ + \text{K}^+ + \text{Mg}^{+2} + \text{Ca}^{+2} + \text{SO}_4^- + \text{HCO}_3^-)/\text{Na}^+$ (Holland, 1978). This
540 approach prevents the inclusion of non-sea salt K^+ , Mg^{+2} , Ca^{+2} , SO_4^- , and HCO_3^- in the sea salt mass and
541 allows for the loss of Cl^- mass through Cl^- depletion processes. It also assumes that all measured Na^+ and
542 Cl^- is derived from seawater. Results of Savoie et al. (1980) indicate that soil dust has a minimal
543 contribution to measured soluble sodium concentrations.

544

545 **3.3.2. Organic and Elemental Carbon**

546 Starting with ACE-Asia in 2001, sub-1 and sub-10 μm samples were collected for OC/EC analysis using
547 2 and 1 stage impactors, respectively (Bates et al., 2004). Each impactor had 2 quartz backup filters. OC
548 concentrations from both impactors were corrected for blanks and artifacts using the last quartz filter in
549 line. Aluminum foil was used as a substrate on the 1.1 μm jet plate. All substrates, aluminum foil and

550 quartz, were prebaked at 500° prior to sampling. One sub-10 µm and one sub-1 µm impactor were
551 operated without a denuder upstream to avoid losses of large particles in the denuder. OC from the sub-
552 1µm impactor was subtracted from the OC from the sub-10 µm impactor to determine supermicron OC
553 concentrations. A second sub-1 µm impactor was operated with a denuder upstream that contained strips
554 of carbon-impregnated glass fiber filters to remove gas phase organics. Sub-1 µm OC and EC were
555 quantified on the impactor samples downstream of the denuder.

556

557 During ACE-Asia and NEAQS 2002, a 7-stage impactor was used for the sampling of OC/EC providing
558 greater size resolution. Aluminum foil substrates were used on all stages of the impactor along with 2
559 quartz backup filters. A 3-stage impactor ($D_{50,aero}$ of 0.18, 1.1, and 10 µm) was used during WACS,
560 WACS-2, and NAAMES-1 through NAAMES-4. These cruises focused on the composition and
561 properties of sea spray aerosol. The 3 size cuts allowed for the separation of the sub-0.18 µm aerosol from
562 larger size ranges in recognition that smaller particle sizes are known to be enriched in organics through
563 the sea spray aerosol production process (Keene et al., 2007).

564

565 OC and EC concentrations on the impactor substrates were measured with a Sunset Labs thermal/optical
566 analyzer (Birch et al., 1996). Four temperature steps were used to achieve a final temperature of 870°C
567 in He to drive off OC. After cooling the sample down to 550°C, a He/O₂ mixture was introduced and the
568 sample was heated in four temperature steps to 910°C to drive off EC. The transmission of light through
569 the filter was measured to separate EC from any OC that charred during the initial stages of heating. No
570 correction was made for carbonate carbon so OC included both organic and inorganic carbon. The mass
571 of particulate organic matter (POM) was determined by multiplying the measured organic carbon
572 concentration in µg m⁻³ by a factor of 2.1 in marine regions and 1.6 elsewhere (Turpin et al., 2001).

573

574 A semi-continuous real-time Sunset Labs thermal/optical analyzer was used during NEAQS 2004 for
575 higher time resolution measurements of OC concentrations. The OC/EC analyzer was downstream of a
576 sub-1 µm impactor and a denuder. The analyzer collected air on a filter for 45 or 105 minutes depending

577 on OC concentrations. At the end of the sampling time the instrument analyzed the filter using the same
578 temperature program described above. The sampling times were not long enough to measure EC above
579 the detection limit of $0.35 \mu\text{g m}^{-3}$.

580

581 **3.3.3. Water soluble organic carbon**

582 A PILS coupled to a Total Organic Carbon (TOC) analyzer (Sievers Model 800 Turbo) was used during
583 TexAQS to measure water soluble organic carbon (WSOC) (Bates et al., 2008). As for the PILS-IC, the
584 PILS-WSOC was connected to the common aerosol inlet but with a stainless steel line. An impactor with
585 a $D_{50,\text{aero}}$ of $1.1 \mu\text{m}$ was upstream of the PILS to sample submicron aerosols. A denuder identical to the
586 one used in the thermal/optical analysis was downstream of the impactor and upstream of the PILS to
587 remove gas phase organics. Two syringe pumps (Kloehn) delivered low-TOC water to the top of the PILS
588 impactor. Two additional pumps were used to pull sample out of the PILS and into the TOC analyzer.
589 The sample was passed through a $0.5 \mu\text{m}$ in-line filter before entering the TOC analyzer to measure
590 WSOC. Between every 45 min to 2 hrs, sample air was passed through a HEPA filter for 15 min to remove
591 particles and determine the measurement background. The measurement background was subtracted from
592 the sample air to obtain ambient WSOC ambient atmospheric concentrations.

593

594 **3.3.4. Trace elements**

595 Starting with AEROSOLS99, sub-1 and sub- $10 \mu\text{m}$ samples were collected for trace element analysis
596 using impactors with a $D_{50,\text{aero}}$ of 1.1 and $10 \mu\text{m}$, respectively (Quinn et al., 2001). Energy Dispersive X-
597 RAY Fluorescence (ED-XRF) was used for quantification (Buck et al., 2021). Both impactors collected
598 aerosol on $2.0 \mu\text{m}$ pore size PALL Teflo Membrane Disc Filters. Supermicron concentrations were
599 determined by subtracting the sub- $1.1 \mu\text{m}$ values from the sub- $10 \mu\text{m}$ values. No corrections were made
600 for particle size or loading. Samples for XRF analysis were collected during all subsequent cruises except
601 for VOCALS, WACS, WACS-2, and NAAMES-1 to 4.

602

603 Concentrations of Al, Si, Ca, Fe, and Ti are included in the NCEI archive as these were used to calculate
604 dust. Other trace elements were measured but were often below detection limit so they were not reported.

605 Dust concentrations were calculated based on measured values of Al, Si, Ca, Fe, and Ti assuming that
606 each element was present in the aerosol in its most common oxide form (Al₂O₃, SiO₂, CaO, K₂O, FeO,
607 Fe₂O₃, TiO₂) (Seinfeld, 1986)). The measured elemental mass concentration was multiplied by the
608 appropriate molar correction factor as shown below (Malm et al., 1994)

609

$$610 \quad \text{Dust} = 2.2(\text{Al}) + 2.49(\text{Si}) + 1.63(\text{Ca}) + 2.42(\text{Fe}) + 1.94(\text{Ti}). \quad (2)$$

611

612 This equation includes a 16% correction factor to account for the presence of oxides of other elements
613 such as K, Na, Mn, Mg, and V that are not included in the linear combination. In addition, the equation
614 omits K from biomass burning by using Fe as a surrogate for soil K and an average K/Fe ratio of 0.6 in
615 soil (Braaten et al., 1986). Non-crustal K was calculated using the K/Al ratio (0.31) of Asian loess (Jahn
616 et al., 2001) which is similar to the ratio in Saharan dust (0.24) and average crustal rock (0.32) (Formenti
617 et al., 2003). Sea salt Ca was accounted for based on the ratio of Ca to Na in seawater.

618

619 **3.3.5. Non-refractory species**

620 Concentrations of submicron non-refractory (NR) NH₄⁺, SO₄⁼, NO₃⁻, and particulate organic matter
621 (POM) were measured on NEAQS 2004, TexAQS, ICEALOT, VOCALS, CalNex, DYNAMO, WACS
622 and WACS-2 with a Quadrupole Aerosol Mass Spectrometer (Q-AMS, Aerodyne Research Inc.,
623 Billerica, MA, USA) (Jayne et al., 2000). The NR species measured by the AMS are defined here as all
624 the chemical components that vaporize at 550°C. The AMS was downstream of an impactor with a D_{50,aero}
625 of 1.1 μm. The ionization efficiency of the AMS was calibrated every few days with dry monodisperse
626 ammonium nitrate particles. Particle losses due to transmission through the aerodynamic lens were
627 corrected by using the DMPS and APS-measured size distributions. Particle losses due to bounce off of
628 the impactor-vaporizer were corrected using simultaneously sampled NH₄⁺ and non-sea salt SO₄⁼
629 concentrations from either the PILS-IC or the impactors (Quinn et al., 2008; Quinn et al., 2006).

630

631 **3.3.6. Aerosol Mass**

632 A filter holder with a Millipore Fluoropore filter (1.0 μm pore size) collected aerosol downstream of a
633 cyclone with a $D_{50,\text{aero}}$ of 1 μm during RITS93 and RITS94. Filters were taken back to PMEL for
634 gravimetric analysis to determine total submicron aerosol mass. The filters were weighed before and after
635 sample collection with a Mettler UMT2 microbalance. The microbalance was housed in a glove box
636 maintained at a constant RH to allow each sampled filter to come into equilibrium with the same vapor
637 pressure of water, thus reducing experimental uncertainty due to a variable lab RH. For RITS93 and
638 RITS94 the RH was maintained at less than 30% by circulating air through a flat baffle box containing a
639 saturated solution of $\text{MgCl}\cdot 6\text{H}_2\text{O}$ and then through the glove box (Young, 1967). The circulated air was
640 cleaned by passing it through a scrubber containing activated charcoal, potassium carbonate, and citric
641 acid. Filters were equilibrated overnight in the glove box prior to weighing. Static charging, which can
642 result in balance instabilities, was minimized by coating the walls of the glove box with a static dissipative
643 polymer (Tech Spray, Inc.), placing an antistatic mat on the glove box floor, and exposing the filters to a
644 ^{210}Po source to dissipate any built-up charge.

645

646 For ACE-1 and the other cruises listed in Table 3, a 2-stage impactor was used to collect submicron and
647 supermicron aerosol for gravimetric analysis. Millipore Fluoropore filter (1.0 μm pore size) and Tedlar
648 films were used for the collection of submicron and supermicron aerosol, respectively. The Tedlar films
649 were cleaned as described in Section 3.3.1. prior to sample collection. Both the Millipore filters and the
650 Tedlar films were weighed before and after sampling. Millipore filters were weighed on the Mettler
651 UMT2 microbalance and Tedlar films were weighed on a Cahn Model 29 microbalance. Both balances
652 were housed in the RH-controlled glove box described above. For cruises with higher sampling RHs of
653 55 to 60% (see Section 3.1.), a saturated solution of KBr was used in the baffle box.

654

655 In addition to the 2-stage impactor used during ACE-Asia, a 7-stage impactor was used for higher size
656 resolution total aerosol mass concentrations.

657

658 All reported mass concentrations include the water mass that is associated with the aerosol on the filter at
659 the glove box RH.

660 *Table 3. Measurements of aerosol chemical composition on each cruise and the instrumentation used.*

Chemical Species and Measurement Method	Size range	Cruise
Inorganic ions		
Inorganic ions ^a Filter with cyclone upstream, IC ^b	Sub-1 μm	MAGE92, RITS93, RITS94
Inorganic ions 2-stage impactor, IC	Sub-1 μm , Supermicron	ACE-1, CSP, ACE-2, AEROSOLS99, INDOEX, NAURU99, ACE-Asia, NEAQS 2002, NEAQS 2004, TexAQS, ICEALOT, VOCALS, CalNex, DYNAMO, WACS, WACS-2, NAAMES-1, NAAMES-2, NAAMES-3, NAAMES-4, ATOMIC
Inorganic ions 7-stage impactor, IC	D _{50,aero} of 0.18, 0.31, 0.55, 1.1, 2.0, 4.1, and 10 μm	All cruises
Inorganic ions PILS ^c , IC	Sub-1 μm	NEAQS 2002, NEAQS 2004, TexAQS
Organic and Elemental Carbon		
OC and EC 2-stage impactor, Thermal analysis ^d	Sub-1 μm , Supermicron	ACE-Asia, NEAQS 2002, NEAQS 2004, TexAQS, ICEALOT, CalNex, ATOMIC
OC and EC Semi-continuous real-time OC/EC with impactor upstream ^e , Thermal analysis	Sub-1 μm	NEAQS 2004
OC and EC 3-stage impactor, Thermal analysis	D _{50,aero} of 0.18, 1.1, and 10 μm	WACS, WACS-2, NAAMES – 1, NAAMES-2, NAAMES-3, NAAMES-4
OC and EC 7-stage impactor, Thermal analysis	D _{50,aero} of 0.18, 0.31, 0.55, 1.1, 2.0, 4.1, and 10 μm	ACE-Asia, NEAQS 2002
WSOC ^f PILS, TOC ^g analyzer	Sub-1 μm	TexAQS
Trace Elements		
Trace Elements ^h 2 impactors, XRF ⁱ	Sub-1 μm ; Sub-10 μm	AEROSOLS99, INDOEX, ACE-Asia, NEAQS 2002, NEAQS 2004, TexAQS, ICEALOT, CalNex, DYNAMO, ATOMIC
Aerosol Mass		
Aerosol mass Filter with cyclone upstream, Gravimetric analysis	Sub-1 μm , Supermicron	RITS93, RITS94
Aerosol mass 2-stage impactor, Gravimetric analysis	Sub-1 μm , Supermicron	ACE-1, ACE-2, AEROSOLS99, INDOEX, ACE-Asia, NEAQS 2002, NEAQS 2004, TexAQS, ICEALOT, VOCALS, CalNex, DYNAMO, WACS, WACS-2, ATOMIC
Non-refractory Species		

NR ^j SO ₄ , NH ₄ , NO ₃ , POM, submicron AMS ^k	Sub-1 μm	NEAQS 2004, TexAQS, ICEALOT, VOCALS, CalNex, DYNAMO, WACS, WACS-2
--	----------	---

- 661 ^aNa⁺, NH₄⁺, K⁺, Ca²⁺, Mg²⁺, Cl⁻, NO₃⁻, SO₄⁼, MSA⁻
662 ^bIon Chromatography
663 ^cParticle-Into-Liquid-Sampler
664 ^dSunset Labs thermal/optical analyzer
665 ^eSunset Labs real-time, semi-continuous thermal/optical analyzer
666 ^fWater Soluble Organic Carbon
667 ^gTotal Organic Carbon Sievers Model 800 Turbo analyzer
668 ^hAl, Si, nss Ca, Ti, Fe
669 ⁱEnergy dispersive X-ray fluorescence
670 ^jNon-refractory
671 ^kAerodyne Mass Spectrometer
672

673 3.4. Aerosol optical Properties

674 The optical properties measured on each cruise and the instrumentation used are listed in Table 4. Aerosol
675 light scattering coefficients were measure on each cruise with the exception of the first one, PSI-91.
676 Variations included measurement at a single wavelength (550 nm) or three wavelengths (450, 550, and
677 700 nm) and measurement of sub-10 micron aerosol or sub-1 and sub-10 micron aerosol. The relative
678 humidity dependence of light scattering, f(RH), was measured on some of the cruises as were
679 backscattering coefficients at 450, 550, and 700 nm.

680

681 Aerosol absorption coefficients were measured on every cruise starting with ACE-1. Initially,
682 measurements were made at 550 nm for sub-10 micron aerosol. These measurements were expanded to
683 sub-1 and sub-10 micron aerosol starting with NAURU99 and 3 wavelengths (467, 530, and 660 nm)
684 starting with NEAQS 2002.

685

686 Aerosol optical depth (AOD) was measured on all cruises except for the first one, PSI-91, with handheld
687 sunphotometers. In addition, the NASA AMES Airborne Tracking sunphotometer (AATS-6) (Livingston
688 et al., 2000) was used during ACE-2.

689

690 Details of the measurements are provided in the following sections.

691

692 **3.4.1. Aerosol Light Scattering**

693 During RITS93 and RITS94, sub-10 micron aerosol light scattering was measured with a newly
694 developed, highly sensitive multiwavelength integrating nephelometer (Bodhaine et al., 1991). This
695 nephelometer, with its high sensitivity, was combined with the closed geometry of the Ahlquist et al.
696 (1967) nephelometer to develop the TSI, Inc. model 3563 (Anderson et al., 1996) that was used during
697 the rest of the cruises reported on here. The enclosed geometry allows for the calibration of the
698 nephelometer with gases with known scattering coefficients.

699

700 The TSI Inc. model 3563 integrating nephelometer was used for all remaining cruises to measure sub-1
701 and sub-10 micron scattering at three wavelengths (450, 550, and 700 nm). Sub-1 and sub-10 micron
702 backscattering were measured on cruises between ACE-1 and WACS. Two single-stage impactors, one
703 having a $D_{50,aero}$ of 1.1 μm and the other of 10 μm were placed upstream of the nephelometer. A valve
704 automatically switched between the two impactors every 15 minutes so that sampling alternated between
705 sub-1 micron and sub-10 micron aerosol. Scattering and backscattering by the supermicron aerosol was
706 determined by difference.

707

708 During all cruises, the nephelometer was calibrated with CO_2 and zeroed with particle-free air every 3 to
709 4 days (Quinn et al., 1996). The resulting zero offset and span factors were applied to the data. In addition,
710 data were corrected for angular nonidealities of the nephelometer, including truncation errors and non-
711 Lambertian illumination using the method of Anderson et al. (1998) or one similar to it.

712

713 The RH of the air sampled by the nephelometer was nominally that of the common inlet as described in
714 Section 3.1. Heating within the nephelometer likely led to slightly lower RH's than for the sizing
715 instruments detailed in Table 2. For ACE-Asia and all subsequent cruises the nephelometer flow path was
716 modified so that the sheath flow was conditioned outside of the instrument case to equilibrate with the
717 temperature-controlled box. It was then reintroduced into the sheath and acceleration nozzle to minimize
718 heating of the sample air and lowering of the measurement RH. In addition, an RH sensor was placed in
719 the nephelometer sensing volume.

720

721 **3.4.2. Relative Humidity Dependence of Light Scattering, $f(\text{RH})$**

722 As indicated in Table 4, the relative humidity dependence of scattering, $f(\text{RH})$, was measured on TexAQS,
723 ICEALOT, VOCALS, CalNex, DYNAMO, WACS, WACS-2, NAAMES-1, NAAMES-2, and
724 ATOMIC. A humidity-controlled system measured light scattering at two different relative humidities,
725 $\sim 20\%$ and $\sim 85\%$, with two nephelometers operated in series downstream of an impactor
726 ($D_{50,\text{aero}} = 1.1 \mu\text{m}$). The first nephelometer in line measured sample air dried with a PermaPure, multiple-
727 tube nafion dryer (model PR-94). Downstream of this nephelometer a humidifier was used to add water
728 vapor to the sample flow using 6 microporous Teflon tubes surrounded by a heated water-jacket.
729 Humidity was measured using a chilled mirror dew point hygrometer downstream of the second
730 nephelometer in line. The same calibration procedure described in Section 3.4.2. was used (Quinn et al.,
731 2022).

732

733 **3.4.3. Aerosol Light Absorption**

734 Between ACE-1 and INDOEX, the aerosol light absorption coefficient of sub- $10 \mu\text{m}$ was measured with
735 a Particle Soot Absorption Photometer (PSAP, Radiance Research) at a wavelength of 550 nm and $\sim 55\%$
736 RH. Measured values were corrected for a scattering artifact, the deposit spot size, flow rate, and the
737 manufacturer's calibration (Bond et al., 1999). Beginning with NAURU99, the absorption coefficient was
738 measured for sub- 1 and sub- $10 \mu\text{m}$ aerosol with the PSAP located downstream of the same impactors as
739 the nephelometer. For NEAQS 2002 and all subsequent cruises, a modified PSAP was used to measure
740 light absorption at three wavelengths (467, 530, and 700 nm) close to that of the TSI nephelometer for
741 calculation of single scattering albedo (Virkkula et al., 2005). Beginning with TexAQS and all following
742 cruises, a PermaPure nafion dryer was placed upstream of the PSAP so that the sample air was at $\sim 25\%$
743 RH. Measurement of dry air was found to reduce instrument noise.

744

745 **3.4.4. Aerosol Optical Depth**

746 Handheld sunphotometers were used to measure AOD for ACE-1 and all subsequent cruises. A single
747 wavelength (550 nm) sunphotometer was used for ACE-1. A microtops unit (Solar Light Co.) was used

748 for all other cruises measuring at 380, 440, 500, 675, and 870 nm. Units were calibrated before each cruise
 749 by either Solar Light Co. or NASA Goddard Space Flight Center (GSFC) using a Langley plot approach
 750 (Shaw, 1983). Initially, a NASA Sensor Intercomparison and Merger for Biological and Interdisciplinary
 751 Oceanic Studies (SIMBIOS) MATLAB routine was used to convert raw signal voltages to AOD. Included
 752 in the conversion is a correction for Rayleigh scattering (Penndorf, 1957) and air mass to account for the
 753 curvature of the Earth (Kasten et al., 1989). Beginning with ICEALOT in 2008, data were reduced as part
 754 of NASA's Maritime Aerosol Network (Smirnov et al., 2009).

755

756 **Table 4. Measurements of aerosol optical properties on each cruise and the instrumentation used.**

Optical Property and Measurement Method	Size Range	Cruise
Scattering		
Scattering (550 nm ^a), Integrating nephelometer	Sub-10 micron	RITS93, RITS94
Scattering (450, 550, 700 nm), Integrating nephelometer, TSI Model 3563	Sub-1 and sub-10 micron	ACE-1, CSP, ACE-2, AEROSOLS99, INDOEX, NAURU99, ACE-Asia, NEAQS 2002, NEAQS 2004, TexAQS, ICEALOT, VOCALS, CalNex, DYNAMO, WACS, WACS-2, NAAMES-1, NAAMES-2, NAAMES-3, NAAMES-4, ATOMIC
Backscattering		
Backscattering (450, 550, 700 nm), Integrating nephelometer, TSI Model 3563	Sub-1 and sub-10 micron	ACE-1, CSP, ACE-2, AEROSOLS99, INDOEX, NAURU99, ACE-Asia, NEAQS 2002, NEAQS 2004, TexAQS, ICEALOT, VOCALS, CalNex, DYNAMO, WACS
Absorption		
Absorption (550 nm), PSAP ^b , Radiance Research	Sub-10 micron	ACE-1, ACE-2, AEROSOLS99, INDOEX
Absorption (550 nm), Sub-1 and PSAP ^b , Radiance Research	Sub-10 micron	NAURU99, ACE-Asia
Absorption (467, 530, 660 nm), PSAP ^b	Sub-1 and sub-10 micron	NEAQS 2002, NEAQS 2004, TexAQS, ICEALOT, VOCALS, CalNex, DYNAMO, WACS, WACS-2, NAAMES-1, NAAMES-2, NAAMES-3, NAAMES-4, ATOMIC
f(RH) scattering and backscattering		
f(RH), scattering and backscattering (450, 550, 700 nm) (25 and 85% RH) 2 Integrating nepelometers, TSI Model 3563	Sub-1 micron	TexAQS, ICEALOT, VOCALS, CalNex, DYNAMO, WACS, WACS-2, NAAMES-1, NAAMES-2, ATOMIC

AOD		
AOD (391, 500 nm) Handheld sunphotometer		RITS93, RITS94
AOD (375, 500, 778, 862 nm) Handheld sunphotometer		ACE-1
AOD (380, 450, 525, 864, 1021 nm) AATS-6 ^c , NASA AMES		ACE-2
AOD (380, 440, 500, 675, 870 nm) Handheld sunphotometer, Solar Light Co. Microtops		AEROSOLS99, INDOEX, NAURU99, ACE-Asia, NEAQS 2002, NEAQS 2004, TexAQS, ICEALOT, VOCALS, CalNex, DYNAMO, WACS, WACS-2, ATOMIC

757

758 ^anm, wavelength

759 ^bParticle Soot Absorption Photometer

760 ^cAmes Airborne Tracking Sunphotometer

761

762 3.5. Gas phase species

763 Gas phase species that were measured include O₃, SO₂, Radon, and DMS. The cruises each gas was
764 measured on and the measurement methods used are listed in Table 5. O₃ and SO₂ were measured
765 primarily as tracers of pollution. Radon (as Rn²²²) was measured as an indicator of contact of the sampled
766 air with land (Whittlestone et al., 1998b). DMS was measured due to its link to nss SO₄⁻ and MSA via
767 oxidation in the atmosphere (e.g. Andreae et al. (1985)).

768

769 3.5.1. Ozone

770 O₃ was measured on all cruises with the exception of NAURU99 and WACS. Three different ozone UV
771 analyzers were used over the years including a Dasibi 1008-AH UV photometer, a TECO Model 49 O₃
772 Analyzer, and a TECO Model 49C O₃ Analyzer (Table 5). For all cruises, a ¼" ID Teflon sample line
773 was used to draw air from the top of the aerosol common sampling mast to the O₃ instrument located in
774 the lab container at the base of the mast. The loss of O₃ in a Teflon sampling line is approximately 5%
775 per 30 m indicating that losses were negligible (< 3%). At intervals of 1 to 4 days, a charcoal filter was
776 placed in the sampling line for 1 hour to determine a zero which was subtracted from the O₃ signal. More
777 details can be found in Johnson et al. (1990).

778

779 **3.5.2. Sulfur dioxide**

780 SO₂ was measured during ACE-Asia, NEAQS 2002, NEAQS 2004, TexAQS, ICEALOT, VOCALS, and
781 CalNex with a Thermo Environmental Instruments Model 43C trace level pulsed fluorescence analyzer.
782 Air was drawn through the 18 m aerosol common sampling mast at 1 m³ min⁻¹. At the base of the mast, a
783 5.0 L min⁻¹ flow was pulled in series through a 1 m long Teflon tube, a Millipore Fluoropore Teflon filter
784 (1.0 μm pore size), a Perma Pure Inc. Nafion dryer (MD-070), a 2 m long Teflon tube, and then into the
785 SO₂ analyzer. The initial 1 m of tubing, filter, and drier were located in the humidity-controlled box at
786 the base of the mast. Dry air was pulled through a charcoal trap and then through the outside of the Nafion
787 dryer at 2 L min⁻¹. The analyzer was run with two channels (0 – 20 ppb full scale and 0 – 100 ppb full
788 scale) and a 20 sec averaging time.

789

790 Zero air (scrubbed with a charcoal trap) was introduced into the sample line upstream of the Fluoropore
791 filter for 10 min every hour to establish a zero baseline. An SO₂ standard was generated with a permeation
792 tube held at 50°C. The flow over the permeation tube, diluted to 17.7 ppb, was introduced into the sample
793 line upstream of the Fluoropore filter for 10 min every 6 hrs (Bates et al., 2004).

794

795 **3.5.3. Radon**

796 The rate of emission of radon from the ocean is ~ 100 times less than over land. As a result, ²²²Rn is a
797 qualitative tracer of an air mass that has been recently influenced by continental emissions (Carlson et al.,
798 1972).

799

800 Radon was measured on all cruises starting with ACE-1 except AEROSOL99, INDOEX, NAURU99,
801 and DYNAMO. Radon (²²²Rn – half-life of 3.82 days) was measured using the two-filter detector method
802 of Whittlestone et al. (1998a). Air is drawn through a HEPA filter which removes all radon and thoron
803 decay products (i.e., daughters), then through a delay chamber in which some daughters are produced.
804 Finally, the air passes through a second filter which retains the daughters. These daughters have been
805 produced in controlled conditions so their number is proportional to the radon concentration. A
806 photomultiplier then counts the radon daughters produced in a 750 L decay tank for a 30-min period. The

807 detector was standardized using radon emitted from a dry radon source (RN-25, PylonElectronics Corp).
808 Background counts were measured under conditions of zero air flow (Quinn et al., 2022).

809

810 **3.5.4. DMS**

811 Air and seawater samples for DMS were analyzed using an automated purge and trap system. Air samples
812 were collected through a Teflon line which ran approximately 60 m from the top of the aerosol sampling
813 mast to the instrument. One hundred mL min⁻¹ of the 4 L min⁻¹ flow were pulled through a KI solution at
814 the instrument to eliminate oxidant interferences (Cooper et al., 1993). The air sample volume ranged
815 from 0.5 to 1.5 L depending on the DMS concentration. Water vapor was removed by passing the flow
816 through a -25°C Teflon tube filled with silanized glass wool. DMS was then trapped in another -25°C
817 Teflon tube filled with Tenax. During the sample trapping period, methylethyl sulfide (MES) was added
818 to the sample stream as an internal standard. At the end of the sampling/purge period, the coolant was
819 pushed away from the trap and the trap was electrically heated. DMS was desorbed onto a DB-1 mega-
820 bore fused silica column where the sulfur compounds were separated isothermally at 50°C quantified with
821 either a Flame Photo Detector (FPD) or a Sulfur Chemiluminescence Detector (SCD). The instrument
822 was calibrated gravimetrically with calibrated permeation tubes. More details of the analysis can be found
823 in Bates et al. (1998b).

824

825 **3.6. Seawater species**

826

827 The cruises each seawater species was measured on and the measurement methods used are listed in Table
828 6.

829

830 **3.6.1. DMS**

831 Seawater samples for DMS analysis were collected from the ship's seawater pumping system at a depth
832 of approximately 5 m below the ship's waterline. Periodically, a 5 mL water sample was valved from the
833 ship's water line into a Teflon gas stripper. The sample was purged with hydrogen for 5 min. DMS and

834 other sulfur gases in the hydrogen purge gas were collected on the Tenax trap held at -25°C as for the air
 835 samples. Seawater and air sample analysis was identical.

836

837 3.6.2. NH₄⁺ and NO₃⁻

838 Seawater samples for the analysis of NH₄⁺ and NO₃⁻ were taken from a depth of ~ 5 m using the ship's
 839 seawater pumping system. Samples were analyzed for NH₄⁺ using the phenolhypochlorite colorimetric
 840 method of Solarzano (1969) and for NO₃⁻ using the method of Parsons et al. (1984). Both of the analyses
 841 were undertaken with a Technicon Autoanalyzer II (Technicon Corp., Tarrytown, New York).

842

843 3.6.3. Chlorophyll-a

844 Discrete seawater samples for chlorophyll-a analysis were taken from the ship's seawater pumping system
 845 2 to 6 times per day. Samples were immediately filtered, put into 10 mL of 90% acetone, and frozen.
 846 Samples were analyzed with a fluorometer within 3 to 4 days onboard the ship. Depending on the cruise,
 847 the fluorometer was calibrated several times during, before, or after the experiment usually with algal
 848 chlorophyll 'a' (Sigma Chemical Corp.). The discrete samples were used to calibrate continuous
 849 fluorescence measurements of seawater also from the ship's underway seawater pumping system.

850

851 *Table 5. Measurements of gas phase species on each cruise and the instrumentation used.*

Parameter and Measurement Method	Cruise
Ozone	
O ₃ Dasibi 1008-AH UV ^a Photometer	PSI-91, MAGE92, RITS93, RITS94, ACE-1, CSP, ACE-2, AEROSOLS99, INDOEX, ACE-Asia, NEAQS 2004
O ₃ TECO Model 49 O ₃ Analyzer	RITS94, ACE-1, CSP, ACE-2, AEROSOLS99, INDOEX, ACE-Asia, NEAQS 2002, NEAQS 2004,
O ₃ TECO Model 49C O ₃ Analyzer	TexAQS, ICEALOT, VOCALS, CalNex, DYNAMO, WACS, WACS-2, NAAMES-1, NAAMES-2, NAAMES-3, NAAMES-4, ATOMIC
SO₂	
SO ₂ TEI Model 43C SO ₂ Analyzer	ACE-Asia, NEAQS 2002, NEAQS 2004, TexAQS, ICEALOT, VOCALS, CalNex
Radon	

Radon (²²² Rn) Two-filter Radon Detector	ACE-1, CSP, ACE-2, ACE-Asia, ACE-Asia, NEAQS 2002, NEAQS 2004, TexAQS, ICEALOT, VOCALS, CalNex, WACS, WACS-2, NAAMES-1, NAAMES-2, NAAMES-3, NAAMES-4, ATOMIC
DMS	
Atmospheric DMS Purge-and-trap system with FPD ^b	MAGE92, RITS93

852 ^aUltra-Violet

853 ^bFlame Photometric Detector

854 ^cSulfur Chemiluminescence Detector

855

856

857 **Table 6. Measurements of seawater species on each cruise and the instrumentation used.**

Parameter and Measurement Method	Cruise
Seawater DMS Purge-and-trap system with FPD	PSI-91, MAGE92, RITS93
Seawater DMS Purge-and-trap system with SCD	RITS94, ACE-1, CSP, ACE-2, AEROSOLS99, INDOEX, ACE-Asia, NEAQS 2004, TexAQS, ICEALOT, VOCALS, CalNex, WACS, WACS-2
Seawater NH ₄ ⁺ Technicon Autoanalyzer II	RITS94
Seawater NO ₃ ⁻ Technicon Autoanalyzer II	PSI-91, RITS93, RITS94, ACE-1, CSP, AEROSOLS99, INDOEX, NAURU99
Seawater Chlorophyll-a Fluorometer	PSI-91, RITS93, RITS94, ACE-1, CSP, ACE-2, AEROSOLS99, INDOEX, NAURU99, CalNex, WACS, WACS-2, NAAMES-1, NAAMES-2, NAAMES-3, NAAMES-4, ATOMIC

858

859

860 **3.7. Ancillary parameters**

861 Ancillary meteorological and seawater parameters were routinely measured on all cruises. These
862 parameters include latitude, longitude, ship's speed and course, true wind speed and direction, relative
863 wind speed and direction, ambient temperature and relative humidity, barometric pressure, and rain rate.
864 Radiosonde data are available for all cruises except PSI-91, MAGE92, RITS93, RITS94, DYNAMO, and
865 WACS. Seawater parameters include sea surface temperature and salinity.

866

867 **4 Summary of Major Findings**

868 Listed below are many of the high-level major findings reported by PMEL based on its global ocean data
869 set of marine aerosol properties. Although they may seem fundamental now, they are a result of early
870 foundational measurements built upon over time with additional cruises in different parts of the world's

871 oceans. These findings were not developed solely by PMEL but along with other pioneering shipboard
872 and aircraft measurements made by many other researchers.

- 873 **1. Measurements of key sulfur species in surface seawater show that most seawater DMS is**
874 **microbially consumed in the water column, while the ocean-to-atmosphere flux of DMS is a**
875 **minor sink in the seawater sulfur cycle** (Bates et al., 1994) (Data from PSI-91).
- 876 **2. The mean surface seawater DMS concentration in the equatorial Pacific (15°S to 15°N) is**
877 **relatively constant seasonally and interannually.** Large interannual variations associated with
878 El Nino – Southern Oscillation (ENSO) events appear to have little effect on the concentration of
879 DMS in tropical surface ocean waters (Bates et al., 1994). (Data from MAGE92, RITS93, RITS94,
880 ACE-1, CSP and previous cruises not described here).
- 881 **3. New particle production in the marine boundary layer is rare** due to the high surface area of
882 sea salt aerosol resulting in the condensation of gas phase precursors onto existing aerosol (Quinn
883 et al., 1993; Covert et al., 1996; Bates et al., 1998b). (Data from PSI-91, MAGE92, RITS93,
884 RITS94, ACE-1).
- 885 **4. The marine aerosol number size distribution has modal characteristics that depend on large**
886 **scale meteorological features and marine boundary layer residence times.** Strong subsidence
887 and entrainment from the FT produce an aerosol dominated by particles in the ultra – fine and
888 Aitken modes (~ 2 to 80 nm). Residence time in the MBL of a few days or more results in a
889 bimodal aerosol with Aitken and accumulation modes (80 to 300 nm in diameter) (Covert et al.,
890 1996; Quinn et al., 1996; Bates et al., 1998b; Bates et al., 2000; Bates et al., 2001; Bates et al.,
891 2002; Quinn et al., 2017). (Data from MAGE92, RITS93, RITS94, ACE-1, ACE-2, AEROSOL99,
892 ICEALOT, WACS-2, NAAMES-1).
- 893 **5. Regional and mesoscale meteorological transport patterns impact aerosol number and**
894 **volume distributions, chemical composition, and optical and cloud-nucleating properties**
895 (Bates et al., 2001; Bates et al., 2002; Bates et al., 2004; Bates et al., 2008; Quinn et al., 2022).
896 (Data from ACE-1, ACE-2, AEROSOLS99, ACE-Asia, NEAQS 2002, NEAQS 2004, TexAQS,
897 ATOMIC).

- 898 6. Sea salt can comprise a significant mass fraction of not only supermicron but also submicron
899 aerosol in the marine atmosphere. Its relatively large mass concentration, high scattering
900 efficiency, and lifetime comparable to other submicron chemical components often results in
901 **submicron sea salt being the dominant contributor to submicron scattering in the marine**
902 **boundary layer** (Quinn et al., 1996; Quinn et al., 1998b; Murphy et al., 1998; Quinn et al., 1999;
903 Quinn et al., 2000; Quinn et al., 2005a). (Data from PSI-91, MAGE92, RITS93, RITS94, ACE-1,
904 ACE-2, AEROSOLS99, INDOEX, ACE-Asia, CSP, NEAQS 2002).
- 905 7. **Instantaneous wind speed often only accounts for a small fraction of the variance in the**
906 **coarse mode number concentration (~30%) and sea salt submicron and supermicron mass**
907 **concentrations (~20 to 78%)** due to variability in upwind conditions and advection to the
908 measurement location (Bates et al., 1998b; Quinn et al., 1999). (Data from PSI-91, MAGE92,
909 RITS93, RITS94, ACE-1).
- 910 8. **A variable and often large fraction of submicron aerosol mass in the marine boundary layer,**
911 **both remote and continentally influenced, is composed of species other than non-sea salt**
912 **sulfate** (McInnes et al., 1996; Quinn et al., 2000; Quinn et al., 2005a). (Data from PSI-91,
913 MAGE92, RITS93, RITS94, ACE-1, ACE-2, AEROSOLS99, INDOEX, ACE-Asia, CSP,
914 NEAQS 2002).
- 915 9. **Sea salt makes up a small fraction of marine boundary layer cloud condensation nuclei**
916 **(Quinn et al., 2017; Quinn et al., 2019). Instead, the CCN population between 70°S and 80°N**
917 **is composed primarily of nss SO₄⁼** due to large-scale meteorological features that result in
918 entrainment of particles from the FT into the MBL and regionally varying MBL aerosol residence
919 times. (Data from RITS93, RITS94, ACE-1, ICEALOT, WACS-2, NAAMES-1, NAAMES-2,
920 NAAMES-3, NAAMES-4).
- 921 10. **Particulate organic matter and its degree of oxidation impacts the relative humidity**
922 **dependence of light scattering and aerosol cloud nucleation** (Quinn et al., 2005b; Quinn et al.,
923 2008). (Results from INDOEX, ACE-Asia, NEAQS 2002, TexAQS).
- 924
925

926 **5 Data Set Usage**

927 Examples of previous uses of the data based on PMEL co-authorship are listed below. Future use of the
928 data is likely to be similar but could be expanded, for example, to halogen chemistry relating to sea spray
929 aerosol.

930

931 **1. Constraints on models and parameterizations** (e.g., Global distribution of sea salt aerosols:
932 new constraints from in situ and remote observations (Jaegle et al., 2011); A review of sea-spray
933 aerosol source functions using a large global set of sea salt aerosol concentration measurements
934 (Gyrthe et al., 2014); Atmospheric sulfur cycle simulated in the global model GOCART'
935 Comparison with field observations and regional budgets (Chin et al., 2000); Modelled radiative
936 forcing of the direct aerosol effect with multi-observation evaluation (Myhre et al., 2009);
937 Numerical study of Asian dust transport during the springtime of 2001 simulated with the
938 Chemical Weather Forecasting System (CFORS) model (Uno et al., 2004); CCN predictions using
939 simplified assumptions of organic aerosol composition and mixing state: a synthesis from six
940 different locations (Ervens et al., 2010); A model for the radiative forcing during ACE-Asia
941 derived from CIRPAS Twin Otter and R/V Ronald H. Brown data and comparison with
942 observations (Conant et al., 2003); Global sea-salt modeling: Results and validation against
943 multicampaign shipboard measurements (Witek et al., 2007); The Global Aerosol Synthesis and
944 Science Project (GASSP) (Reddington et al., 2017)).

945

946 **2. Intercomparison of instruments and methods** (e.g., ACE-Asia intercomparison of a thermal-
947 optical method for the determination of particle-phase organic and elemental carbon (Schauer et
948 al., 2003); Bias in filter based aerosol absorption measurements due to organic aerosol loading:
949 Evidence from ambient measurements (Lack et al., 2008); Comparison of aerosol single scattering
950 albedos derived by diverse techniques in two North Atlantic experiments (Russell et al., 2002)).

951

952 **3. Comparison to and validation of remote retrievals** (e.g., Measurements of aerosol vertical
953 profiles and optical properties during INDOEX 1999 using micropulse lidars (Welton et al., 2002);

954 Geostationary satellite retrievals of aerosol optical thickness during ACE-Asia (Wang et al.,
955 2003); Clear-sky infrared aerosol radiative forcing at the surface and the top of the atmosphere
956 (Markovic et al., 2003); Spectral absorption of solar radiation by aerosols during ACE-Asia
957 (Bergstrom et al., 2004); Lidar measurements during Aerosols99 (Voss et al., 2001); Multi-grid-
958 cell validation of satellite aerosol property retrievals in INTEX/ITCT/ICARTT 2004 (Russell et
959 al., 2007); Shipboard sunphotometer measurements of aerosol optical depth spectra and columnar
960 water vapor during ACE 2 and comparison with selected land, ship, aircraft, and satellite
961 measurements).

962

963 **4. Addition to larger data sets** (e.g., Maritime aerosol network as a component of aerosol robotic
964 network (Smirnov et al., 2009); Total observed organic carbon (TOOC) in the atmosphere: a
965 synthesis of North American observations (Heald et al., 2008); A global database of sea surface
966 DMS measurements and a simple model to predict sea surface DMS as a function of latitude,
967 longitude and month (Kettle et al., 1999)).

968

969 **6 Summary**

970 PMEL conducted 25 cruises between 1991 and 2020 measuring aerosol chemical, microphysical, optical,
971 and cloud nucleating properties. These cruises provide coverage in all of the world's oceans resulting in
972 the largest global ocean data set of marine aerosol properties. The data set also includes gas phase and
973 seawater species. PMEL's major findings and data usage by others are summarized. A description of each
974 cruise is provided including location, timing, and objectives. References are cited to provide a deeper
975 context for each cruise. The intention of the paper is to advance widespread use of the data by the broader
976 research community.

977

978 **7 Data availability**

979 All cruise data sets are publicly available at NOAA's National Centers for Environmental Information
980 (<https://www.ncei.noaa.gov>). Cruise identification, data links (DOIs), and data references are provided
981 in Table 6. The data are permanently and publicly available at NCEI.

982

983 **Table 6. Summary of cruise data links (DOIs), and references. See Table 1 for dates, ports, and ocean**
 984 **region for each cruise. The data are permanently and publicly available at NOAA's NCEI.**

985

Cruise	Data links	Data reference
PSI-91	https://doi.org/10.25921/44nn-d608	(Quinn et al., 2026c)
MAGE92	https://doi.org/10.25921/bz8f-b917	(Quinn et al., 2026k)
RITS93	https://doi.org/10.25921/ec4p-9410	(Quinn et al., 2026h)
RITS94	https://doi.org/10.25921/ec4p-9410	(Quinn et al., 2026h)
ACE-1 Leg 1	https://doi.org/10.25921/z3bm-y330	(Quinn et al., 2026g)
ACE-1 Leg 2	https://doi.org/10.25921/z3bm-y330	(Quinn et al., 2026g)
CSP	https://doi.org/10.25921/pgzy-5h08	(Quinn et al., 2026f)
ACE-2	https://doi.org/10.25921/3fk0-0m36	(Quinn et al., 2025f)
AEROSOLS99	https://doi.org/10.25921/67kx-2d82	(Quinn et al., 2026b)
INDOEX	https://doi.org/10.25921/67kx-2d82	(Quinn et al., 2026b)
NAURU99	https://doi.org/10.25921/e2rz-yg88	(Quinn et al., 2026i)
ACE-Asia	https://doi.org/10.25921/jd13-t245	(Quinn et al., 2026j)
NEAQS 2002	https://doi.org/10.25921/q66h-r438	(Quinn et al., 2026l)
NEAQS 2004	https://doi.org/10.25921/q66h-r438	(Quinn et al., 2026l)
TexAQS-GoMACCS	https://doi.org/10.25921/c6n1-0840	(Quinn et al., 2025a)
ICEALOT	https://doi.org/10.25921/bgy4-3075	(Quinn et al., 2025c)
VOCALS	https://doi.org/10.25921/mafn-2n04	(Quinn et al., 2025e)
CalNex	https://doi.org/10.25921/xf4m-dx08	(Quinn et al., 2025b)
DYNAMO	https://doi.org/10.25921/m0ec-rn58	(Quinn et al., 2026e)
WACS	https://doi.org/10.25921/tx5t-1e17	(Quinn et al., 2026d)
WACS2	https://doi.org/10.25921/tx5t-1e17	(Quinn et al., 2026d)
NAAMES1	https://doi.org/10.25921/df6d-p183	(Quinn et al., 2025d)
NAAMES2	https://doi.org/10.25921/df6d-p183	(Quinn et al., 2025d)
NAAMES3	https://doi.org/10.25921/df6d-p183	(Quinn et al., 2025d)
NAAMES4	https://doi.org/10.25921/df6d-p183	(Quinn et al., 2025d)

ATOMIC	https://doi.org/10.25921/w7ab-3s87	(Quinn et al., 2026a)
--------	---	-----------------------

986

987

988

989 **Author contributions**

990 T.S.B. and P.K.Q. conceptualized research goals. P.K.Q., T.S.B., D.J.C., J.E.J., and L.M.U. participated
991 in collecting and analyzing data. P.K.Q. prepared the paper. D.J.C. and H.B. prepared data sets for
992 archival at NCEI.

993

994 **Competing interests**

995 The authors declare that they have no conflict of interest.

996

997 **Acknowledgments**

998 We thank the crews of the NOAA *R/Vs* Discoverer, Surveyor, and Ronald H. Brown; USC *R/V* Vickers;
999 the IBSS *R/V* Professor Vodyanitiskiy; and UNOLS *R/Vs* Atlantis, Roger Revelle, and Knorr who made
1000 this work possible. This is PMEL contribution number 5806.

1001

1002 **Financial support**

1003 Funding was provided over the years by NOAA's Climate and Global Change Program, New England
1004 Air Quality Study, Health of the Atmosphere Program, Climate Program Office, and Oceanic and
1005 Atmospheric Research Office; NASA's Interdisciplinary Studies Program, Mission to Planet Earth
1006 Science Division, Global Aerosol Climatology Project, and Earth System Science Program; the NSF
1007 Atmospheric Chemistry Program; and the Office of Naval Research.

1008

1009 **References**

1010

1011 Ahlquist, N. C. and Charlson, R. J.: A new instrument for evaluating the visual quality of air, *Journal of*
1012 *the Air Pollution Control Association*, 17, 467 - 469., 1967.

1013 Aller, J., Radway, J. C., Kiltbau, W. P., Bothe, D. W., Wilson, T. W., Vaillancourt, R. D., Quinn, P. K.,
1014 Coffman, D. J., et al.: Size-resolved characterization of the polysaccharided and proteinaceous
1015 components of seawater, *Atmospheric Environment*, 154, 331 - 347, 2017.

1016 Anderson, T. L. and Ogren, J.: Determining aerosol radiative properties using the TSI 3563 integrating
1017 nephelometer, *Aerosol Science and Technology*, 29, 57 - 69, 1998.

1018 Anderson, T. L., Covert, D. S., Marshall, S. F., Laucks, M. L., Charlson, R. J., Waggoner, A. P., Ogren,
1019 J., Caldow, R., et al.: Performance characteristics of a high-sensitivity, three-wavelength total
1020 scatter/backscatter nephelometer, *Journal of Atmospheric and Oceanic Technology*, 13, 967 - 986,
1021 1996.

1022 Andreae, M. O., Ferek, R. J., Bermond, F., Byrd, K. P., Engstrom, T., Hardin, S., Houmère, P. D.,
1023 LeMarrec, F., et al.: Dimethyl sulfide in the marine atmosphere, *Journal of Geophysical Research -*
1024 *Atmosphere*, 90, 12,891 - 812,900, 1985.

1025 Bates, T. S., Coffman, D. J., Covert, D. S., and Quinn, P. K.: Regional marine boundary layer aerosol
1026 size distributions in the Indian, Atlantic and Pacific Oceans: A comparison of INDOEX measurements
1027 with ACE-1 and ACE-2, and Aerosols99, *Journal of Geophysical Research - Atmospheres*, 107, 8026,
1028 2002.

1029 Bates, T. S., Quinn, P. K., Coffman, D. J., and Johnson, J. E.: The Dominance of Organic Aerosols in
1030 the Marine Boundary Layer over the Gulf of Maine during NEAQS 2002 and their Role in Aerosol
1031 Light Scattering, *Journal of Geophysical Research - Atmosphere*, 110, doi:10.1029/2005JD005797,
1032 2005.

1033 Bates, T. S., Huebert, B. J., Gras, J., Griffiths, F. B., and Durkee, P. A.: International Global
1034 Atmospheric Chemistry (IGAC) Projects' First Aerosol Characterization Experiment (ACE 1):
1035 Overview, *Journal of Geophysical Research - Atmosphere*, 103, 16,297 - 216,318, 1998a.

1036 Bates, T. S., Quinn, P. K., Coffman, D. J., Johnson, J. E., Miller, T. L., and Covert, D. S.: Regional
1037 physical and chemical properties of the marine boundary layer aerosol across the Atlantic during
1038 Aerosols99: An overview, *Journal of Geophysical Research - Atmosphere*, 106, 20,767 - 720,782, 2001.

1039 Bates, T. S., Quinn, P. K., Coffman, D. J., Schulz, K., Covert, D. S., and Johnson, J. E.: Boundary Layer
1040 Aerosol Chemistry during TexAQS/GoMACCS 2006: Insights into Aerosol Sources and
1041 Transformation Processes, *Journal of Geophysical Research - Atmosphere*, 113,
1042 doi:10.1029/2008JD010023, 2008.

1043 Bates, T. S., Quinn, P. K., Covert, D. S., Coffman, D. J., Johnson, J. E., and Wiedensohler, A.: Aerosol
1044 physical properties and processes in the lower marine boundary layer: A comparison of shipboard sub-
1045 micron data from ACE-1 and ACE-2, *Tellus*, 52B, 258 - 272, 2000.

1046 Bates, T. S., Kiene, R. P., Wolfe, G. V., Matrai, P. A., Chavez, F. P., Buck, K. R., Blomquist, B. W.,
1047 and Cuhel, R. L.: The cycling of sulfur in surface seawater of the northeast Pacific, *Journal of*
1048 *Geophysical Research - Atmospheres*, 99, 7835 - 7843, 1994.

1049 Bates, T. S., Kapustin, V. N., Quinn, P. K., Covert, D. S., Coffman, D. J., Mari, C., Durkee, P. A., De
1050 Bruyn, W., and Saltzman, E. S.: Processes controlling the distribution of aerosol particles in the lower
1051 marine boundary layer during the First Aerosol Characterization Experiment (ACE 1), *Journal of*
1052 *Geophysical Research - Atmosphere*, 103, 16,369 - 316,383, 1998b.

1053 Bates, T. S., Quinn, P. K., Coffman, D. J., Covert, D. S., Miller, T. L., Johnson, J. E., Carmichael, G.
1054 R., Guazotti, S. A., et al.: Marine boundary layer dust and pollution transport associated with the
1055 passage of a frontal system over eastern Asia, *Journal of Geophysical Research - Atmosphere*, 109,
1056 doi:10.1029/2003JD004094, 2004.

1057 Bates, T. S., Quinn, P. K., Frossard, A. A., Russell, L. M., Hakala, J., Petaja, T., Kulmala, M., Covert,
1058 D. S., et al.: Measurements of ocean derived aerosol off the coast of California, *Journal of Geophysical*
1059 *Research-Atmospheres*, 117, Artn D00v15
1060 Doi 10.1029/2012jd017588, 2012.

1061 Behrenfeld, M. J., Moore, R. H., Hostetler, C. A., Graff, J., Gaube, P., Russell, L. M., Chen, G., Doney,
1062 S. C., et al.: The North Atlantic aerosol and marine ecosystem study (NAAMES): Science motive and
1063 mission overview, *Frontiers of Marine Science*, 22, doi.org/10.3389/fmars.2019.00122, 2019.

1064 Berg, O. H., Swietlicki, E., and Krejci, R.: Hygroscopic growth of the aerosol particles in the marine
1065 boundary layer over the Pacific and Southern Oceans during the First Aerosol Characterization
1066 Experiment (ACE 1), *Journal of Geophysical Research - Atmosphere*, 103, 16,535 - 516,546, 1998.

1067 Bergstrom, R. W., Pilewskie, P., Schmid, B., Redemann, J., Russell, P. B., Hirasgashi, A., Nakajima, T.,
1068 and Quinn, P. K.: Spectral absorption of solar radiation by aerosols during ACE-Asia, *Journal of*
1069 *Geophysical Research - Atmosphere*, 109, doi:10.1029/2003JD004467, 2004.

1070 Berner, A., Lurzer, C., Pohl, F., Preining, O., and Wagner, P.: The size distribution of the urban aerosol
1071 in Vienna, *Science of the Total Environment*, 13, 245 - 261, 1979.

1072 Birch, M. E. and Cary, R. A.: Elemental carbon-based method for monitoring occupational exposures to
1073 particulate diesel exhaust, *Aerosol Science and Technology*, 25, 221 - 241, 1996.

1074 Bodhaine, B. A., Alhquist, N. C., and Schnell, R. C.: Three-wavelength nephelometer suitable for
1075 aircraft measurements os background aerosol scattering extinction coefficient, *Atmospheric*
1076 *Environment*, 25A, 2267 - 2276, 1991.

1077 Bond, T. C., Anderson, T. L., and Campbell, D.: Calibration and intercomparison of filter-based
1078 measurements of visible light absorption by aerosols, *Aerosol Science and Technology*, 30, 582 - 600,
1079 1999.

1080 Braaten, D. A. and Cahill, T. A.: Size and composition of Asian dust transported to Hawaii,
1081 *Atmospheric Environment*, 20, 1105 - 1109, 1986.

1082 Buck, N. J., Barrett, P. M., Morton, P. L., Landing, W. M., and Resing, J. A.: Energy dispersive X-ray
1083 fluorescence methodology and analysis of suspended particulate matter in seawater for trace element
1084 compositions and an intercomparison with high-resolution inductively coupled plasma-mass
1085 spectrometry, *Limnology and Oceanography: Methods*, 19, 401 - 415, 2021.

1086 Carlson, T. N. and Prospero, J. M.: The large-scale movement of Saharan air outbreaks over the
1087 northern equatorial Atlantic, *Journal of Applied Meteorology*, 11, 283 - 297, 1972.

1088 Carrico, C. M., Kus, P., Rood, M. J., Quinn, P. K., and Bates, T. S.: Mixtures of pollution, dust, sea salt,
1089 and volcanic aerosol during
1090 ACE-Asia: Aerosol radiative properties as a function of relative humidity, *Journal of Geophysical*
1091 *Research - Atmosphere*, 108, doi:10.1029/2003JD003405, 2003.

1092 Charlson, R. J., Poeschel, R. F., and Horvath, H.: The direct measurement of atmospheric light
1093 scattering coefficient for studies of visibility and air pollution, *Atmospheric Environment*, 1, 469 - 478,
1094 1967.

1095 Chin, M., Savoie, D. L., Huebert, B. J., Bandy, A. R., Thornton, D. C., Bates, T. S., Quinn, P. K.,
1096 Saltzman, E. S., and De Bruyn, W.: Atmospheric sulfur cycle simulated in the global model GOCART:
1097 Comparison with field observations and regional budgets, *Journal of Geophysical Research -*
1098 *Atmosphere*, 105, 24,689 - 624,712, 2000.

1099 Clarke, A. D., Freitag, S., Simpson, R. M. C., Hudson, J. G., Howell, S. G., V.L., B., Campos, T., and
1100 Kapustin, V. N.: Free troposphere as a major source of CCN for the equatorial pacific boundary layer:
1101 long-range transport and teleconnections, *Atmospheric Chemistry and Physics*, 13, 7511 - 7529, 2013.

1102 Conant, W. C., Seinfeld, J. H., Wang, J., Carmichael, G. R., Tang, Y., Uno, I., Flatau, P. J., Markowicz,
1103 K. M., and Quinn, P. K.: A model for the radiative forcing during ACE-Asia derived from CIRPAS

1104 Twin Otter and R/V Ronald H. Brown data and comparison with observations, *Journal of Geophysical*
1105 *Research - Atmosphere*, 108, doi:10.1029/2002JD003260, 2003.

1106 Cooper, D. J. and Saltzman, E. S.: Measurements of atmospheric dimethylsulfide, hydrogen sulfide, and
1107 carbon disulfide during GTE/CITE 3, *Journal of Geophysical Research - Atmosphere*, 98, 23,397 -
1108 323,410, 1993.

1109 Corbett, J. J., Winebrake, J. J., Green, E. H., Kasibhatla, P., Eyring, V., and Lauer, A.: Mortality from
1110 ship emissions: A global assessment, *Environmental Science & Technology*, 41, 8512-8518, Doi
1111 10.1021/Es071686z, 2007.

1112 Covert, D. S., Wiedensohler, A., and Russell, L. M.: Particle charging and transmission efficiencies of
1113 aerosol charge neutralizers, *Aerosol Science and Technology*, 27, 206 - 214, 1997.

1114 Covert, D. S., Kapustin, V. N., Bates, T. S., and Quinn, P. K.: Physical properties of marine boundary
1115 layer aerosol particles of the mid-Pacific in relation to sources and meteorological transport, *Journal of*
1116 *Geophysical Research - Atmosphere*, 101, 6919 - 6930, 1996.

1117 Covert, D. S., Kapustin, V. N., Quinn, P. K., and Bates, T. S.: New particle formation in the marine
1118 boundary layer, *Journal of Geophysical Research - Atmosphere*, 97, 20,581 - 520,590, 1992.

1119 de Leeuw, G., Andreas, E. L., Anguelova, M. D., Fairall, C. W., Lewis, E. R., O'Dowd, C., Schulz, M.,
1120 and Schwartz, S. E.: Production Flux of Sea Spray Aerosol, *Reviews of Geophysics*, 49, Rg2001,
1121 10.1029/2010rg000349, 2011.

1122 DeWitt, H. L., Coffman, D. J., Schulz, K. J., Brewer, A., Bates, T. S., and Quinn, P. K.: Atmospheric
1123 aerosol properties over the equatorial Indian Ocean and the impact of the Madden-Julia Oscillation,
1124 *Journal of Geophysical Research - Atmospheres*, 118, 10.1002/jgrd.50419, 2013.

- 1125 Ervens, B., Cubison, M. J., Andrews, E., Feingold, G., Ogren, J., Jimenez, J., Quinn, P. K., Bates, T. S.,
1126 et al.: CCN predictions using simplified assumptions of organic aerosol composition and mixing state: a
1127 synthesis from six different locations, *Atmospheric Chemistry and Physics*, 10, 4795 - 4807, 2010.
- 1128 Fehsenfeld, F. C., Ancellet, G., Bates, T. S., Goldstein, A. J., Hardesty, R. M., Honrath, R., Law, K. S.,
1129 Lewis, A. C., et al.: International Consortium for Atmospheric Research on Transport and
1130 Transformation (ICARTT): North America to Europe —Overview of the 2004 summer field study,
1131 *Journal of Geophysical Research - Atmospheres*, 111, 10.1029/2006JD0078729, 2006.
- 1132 Formenti, P., Elbert, W., Maenhaut, W., Haywood, J., and Andreae, M. O.: Chemical composition of
1133 mineral dust aerosol during the Saharan Dust Experiment (SHADE) airborne campaign in the Cape
1134 Verde region, September 2000, *Journal of Geophysical Research - Atmosphere*, 108,
1135 <https://doi.org/10.1029/2002JD002648>, 2003.
- 1136 Gyrthe, H., Strom, J., Krejci, R., Quinn, P. K., Coffman, D. J., and Eck, T. F.: A review of seaspray
1137 aerosol source functions using a large global set of sea salt aerosol concentration measurements,
1138 *Atmospheric Chemistry and Physics*, 14, 1277 - 1297, 2014.
- 1139 Hawkins, L. N. and Russell, L. M.: Polysaccharides, Proteins, and Phytoplankton Fragments: Four
1140 Chemically Distinct Types of Marine Primary Organic Aerosol Classified by Single Particle
1141 Spectromicroscopy, *Advances in Meteorology*, 612132, 10.1155/2010/612132, 2010.
- 1142 Heald, C. L., Goldstein, A. H., Allan, J., Aiken, A. C., Apel, E., Atlas, E. L., Baker, A. K., Bates, T. S.,
1143 et al.: Total observed organic carbon (TOOC) in the atmosphere: a synthesis of North American
1144 observations, *Atmospheric Chemistry and Physics*, 8, 2007 - 2025, 2008.
- 1145 Holland, H. D.: *The Chemistry of the Atmosphere and Oceans*, John Wiley, New York 1978.

1146 Huebert, B. J., Bates, T. S., Russell, P. B., Shi, G., Kim, Y. J., Kawamura, K., Carmichael, G., and
1147 Nakajima, T.: An overview of ACE-Asia: Strategies for quantifying the relationships between Asian
1148 aerosols and their climatic impacts, *Journal of Geophysical Research - Atmospheres*, 108,
1149 10.1029/2003JD003550, 2003.

1150 Jaegle, L., Quinn, P. K., Bates, T. S., Alexander, B., and Lin, J. T.: Global distribution of sea salt
1151 aerosols: new constraints from in situ and remote sensing observations, *Atmospheric Chemistry and
1152 Physics*, 11, 3137-3157, DOI 10.5194/acp-11-3137-2011, 2011.

1153 Jahn, B.-M., Gallet, S., and Han, J.: Geochemistry of the Xining, Xifeng and Jixian section, Loess
1154 Plateau of China: Eolian dust
1155 provenance and paleosol evolution during the last 140 k, *Chemical Geology*, 178, 71 - 94, 2001.

1156 Jayne, J. T., Leard, D. C., Zhang, X., Davidovits, P., Smith, K. A., Kolb, C. E., and Worsnop, D. R.:
1157 Development of an aerosol mass spectrometer for size and composition analysis of submicron particles,
1158 *Aerosol Science and Technology*, 33, 49 - 70, 2000.

1159 Johnson, J. E., Gammon, R. H., Larsen, J., Bates, T. S., Oltmans, S. L., and Farmer, J. C.: Ozone in the
1160 marine boundary layer over the Pacific and Indian Oceans: Latitudinal Gradients and Diurnal Cycles,
1161 *Journal of Geophysical Research - Atmosphere*, 95, 11,847 - 811,856, 1990.

1162 Kastner, F. and Young, A. T.: Revised optical air mass tables and approximation formula, *Applied
1163 Optics*, 28, 4735 - 4738, 1989.

1164 Kaufman, Y. J., Koren, I., Remer, L., Tanre, D., Ginoux, P., and Fan, S.: Dust transport and deposition
1165 observed from the Terra-Moderate Resolution Imaging Spectroradiometer (MODIS) spacecraft over the
1166 Atlantic Ocean
1167 , *Journal of Geophysical Research - Atmospheres*, 110, doi:10.1029/2003JD004436, 2005.

1168 Kawamura, K., Hoque, M., Bates, T. S., and Quinn, P. K.: Molecular distributions and isotopic
1169 compositions of organic aerosols over the western North Atlantic: Dicarboxylic acids, related
1170 compounds, sugars and secondary organic aerosol tracers, *Organic Geochemistry*, 113, 229 - 238, 2017.

1171 Keady, P. B., Quant, F. R., and Sem, G. S.: Differential mobility particle sizer: A new instrument for
1172 high resolution aerosol size distribution measurements below 1 micron, *TSI Q.*, 9, 3 - 11, 1983.

1173 Keene, W. C., Long, M. S., Reid, J. S., Frossard, A. A., Kieber, D. J., Maben, J., Russell, L. M., Kinsey,
1174 J. D., et al.: Factors that modulate properties of primary marine aerosol generated from ambient
1175 seawater on ships at sea, *Journal of Geophysical Research - Atmospheres*, 122, 11,961 - 911,990, 2017.

1176 Keene, W. C., Maring, H., Maben, J. R., Kieber, D. J., Pszenny, A. A. P., Dahl, E. E., Izaguirre, M. A.,
1177 Davis, A. J., et al.: Chemical and physical characteristics of nascent aerosols produced by bursting
1178 bubbles at a model air-sea interface, *Journal of Geophysical Research-Atmospheres*, 112, D21202,
1179 10.1029/2007jd008464, 2007.

1180 Kettle, A. J., Andreae, M. O., Amouroux, D., Andreae, T. W., and Bates, T. S.: A global database of sea
1181 surface dimethylsulfide (DMS) measurements and a simple model to predict sea surface DMS as a
1182 function of latitude, longitude and month, *Global Biogeochemical Cycles*, 13, 399 - 444, 1999.

1183 Lack, D. A., Cappa, C. D., Covert, D. S., Baynard, T., Passoli, P., Sierau, G., Bates, T. S., Quinn, P. K.,
1184 et al.: Bias in filter based aerosol absorption measurements due to organic aerosol loading: Evidence
1185 from ambient measurements, *Journal of Aerosol Science and Technology*, 42,
1186 doi:10.1080/02786820802389277, 2008.

1187 Li, J., Carlson, B. E., Yung, Y. L., Lv, D., Hansen, J., Penner, J., Liao, H., Ramaswamy, V., et al.:
1188 Scattering and absorbing aerosols in the climate system, *Nature Reviews Earth and Environment*, 3, 363
1189 - 379, 2022.

1190 Liu, B. Y. H. and Lee, K. W.: Efficiency of membrane and Nuclepore filters for submicrometer
1191 aerosols, *Environmental Science and Technology*, 10, 345 - 350, 1976.

1192 Livingston, J. M., Kapustin, V. N., Schmid, B., Russell, P. B., Quinn, P. K., Bates, T. S., Durkee, P. A.,
1193 Smith, P. J., et al.: Shipboard sunphotometer measurements of aerosol optical depth spectra and
1194 columnar water vapor during ACE-2 and comparison with selected land, ship, aircraft, and satellite
1195 measurements, *Tellus*, 52B, 594 - 619, 2000.

1196 Logan, T., Xi, B., Dong, X., Obrecht, R., Li, Z., and Cribb, M.: A study of Asian dust plumes using
1197 satellite, surface, and aircraft measurements during the INTEX-B field experiment, *Journal of*
1198 *Geophysical Research - Atmospheres*, 115, doi.org/10.1029/2010JD014134, 2010.

1199 Malm, W. C., Sisler, J. F., Huffman, D., Eldred, R. A., and Cahill, T. A.: Spatial and seasonal trends in
1200 particle concentration and optical extinction in the United States, *Journal of Geophysical Research -*
1201 *Atmosphere*, 99, 1347 - 1370, 1994.

1202 Markovic, M. Z., Flatau, P. J., Vogelmann, A. M., Quinn, P. K., and Welton, E. J.: Clear-sky infrared
1203 aerosol radiative forcing at the surface and the top of the atmosphere, *Quarterly Journal of the Royal*
1204 *Meteorological Society*, 129, 2927 - 2948, 2003.

1205 McInnes, L. M., Quinn, P. K., Covert, D. S., and Anderson, T. L.: Gravimetric analysis, ionic
1206 composition, and associated water mass of the marine aerosol, *Atmospheric Environment*, 30, 869 -
1207 884, 1996.

1208 Murphy, D. M., Anderson, J. R., Quinn, P. K., McInnes, L. M., Brechtel, F. J., Kreidenweis, S. M.,
1209 Middlebrook, A. M., Posfai, M., et al.: Influence of sea-salt on aerosol radiative properties in the
1210 Southern Ocean marine boundary layer, *Nature*, 392, 62-65, 1998.

1211 Myhre, G., Berglen, T. F., Johnsrud, M., Hoyle, C. R., Bernsten, T. K., Christopher, S. A., Fahey, D.
1212 W., Isaksen, I., et al.: Modelled radiative forcing of the direct aerosol effect with multi-observation
1213 evaluation, *Atmospheric Chemistry and Physics*, 9, 1365 - 1392, 2009.

1214 Parrish, D. D., Allen, D. T., Bates, T. S., Estes, M., Fehsenfeld, F. C., Feingold, F., Ferrare, R.,
1215 Hardesty, R. M., et al.: Overview of the second Texas air quality study (TexAQS II) and the Gulf of
1216 Mexico atmospheric composition and climate study (GoMACCS), *Journal of Geophysical Research -*
1217 *Atmospheres*, 114, doi:10.1029/2009JD011842, 2009.

1218 Parsons, T. R., Maita, Y., and Lalli, C. M.: *A Manual of Chemical and Biological Methods for Seawater*
1219 *Analysis*, Pergamon, New York 1984.

1220 Penndorf, R.: Tables of refractive index for standard air and the Rayleigh scattering coefficient for the
1221 spectral region between 0.2 and 20 μm and their application to atmospheric optics, *Journal of the*
1222 *Optical Society of America*, 47, 176 - 182, 1957.

1223 Post, M. J. and Fairall, C. W.: Early results from the Nauru99 campaign on NOAA ship Ronald H.
1224 Brown, *IGARS 2000*, 110.1109/IGARSS.2000.85802,

1225 Post, M. J., Fairall, C. W., J.R., S., Han, Y., White, A. B., Ecklund, W. L., Weickmann, A., Quinn, P.
1226 K., et al.: The combined sensor program: an air-sea science mission in the central and western Pacific
1227 Ocean, *Bulliten of the American Meteorological Society*, 78, 2797 - 2815, 1997.

1228 Quinn, P. K. and Bates, T. S.: Regional aerosol properties: Comparisons of boundary layer
1229 measurements from ACE 1, ACE 2, Aerosols99, INDOEX, ACE Asia, TARFOX, and NEAQS, *Journal*
1230 *of Geophysical Research - Atmosphere*, 110, doi: 10/1024/2004JD004755, 2005a.

1231 Quinn, P. K. and Coffman, D. J.: Local closure during ACE 1: Aerosol mass concentration and
1232 scattering and backscattering coefficients, *Journal of Geophysical Research - Atmosphere*, 109, 16575 -
1233 16596, 1998a.

1234 Quinn, P. K. and Coffman, D. J.: Comment on "Contribution of different aerosol species to the global
1235 aerosol extinction optical thickness: Estimates from model results" by Tegen et al., *Journal of*
1236 *Geophysical Research-Atmospheres*, 104, 4241-4248, Doi 10.1029/1998jd200066, 1999.

1237 Quinn, P. K., Bates, T. S., and Coffman, D. J.: Texas Air Quality - Gulf of Mexico Atmospheric
1238 Composition and Climate Study (TexAQS/GoMACCS): Physical, optical, and chemical properties of
1239 atmospheric marine aerosols aboard NOAA R/V Ronald H. Brown in the Gulf of America, 2006-07-27
1240 to 2006-09-12 (NCEI Accession 0310784). NOAA National Centers for Environmental Information.
1241 [dataset], <https://doi.org/10.25921/c6n1-0840>, 2025a.

1242 Quinn, P. K., Bates, T. S., and Coffman, D. J.: California Research at the Nexus of Air Quality and
1243 Climate Change (CalNex) Field Campaign: Physical, optical, and chemical properties of atmospheric
1244 marine aerosols aboard WHOI R/V Atlantis along the California coast, 2010-05-14 to 2010-06-09
1245 (NCEI Accession 0310783). NOAA National Centers for Environmental Information. [dataset],
1246 <https://doi.org/10.25921/xf4m-dx08>, 2025b.

1247 Quinn, P. K., Bates, T. S., and Coffman, D. J.: International Chemistry Experiment in the Arctic Lower
1248 Troposphere (ICEALOT): Physical, optical, and chemical properties of atmospheric marine aerosols
1249 aboard WHOI R/V Knorr in Arctic ice-free regions of the Greenland, Norwegian, and Barents seas,
1250 2008-03-19 to 2009-04-24 (NCEI Accession 0310737). NOAA National Centers for Environmental
1251 Information. [dataset], <https://doi.org/10.25921/bgy4-3075>, 2025c.

1252 Quinn, P. K., Bates, T. S., and Coffman, D. J.: North Atlantic Aerosols and Marine Ecosystems Study
1253 (NAAMES): Physical, optical, and chemical properties of atmospheric marine aerosols aboard WHOI

1254 R/V Atlantis in the western subarctic North Atlantic, 2015 to 2018 (NCEI Accession 0310822). NOAA
1255 National Centers for Environmental Information. [dataset], <https://doi.org/10.25921/df6d-p183>, 2025d.

1256 Quinn, P. K., Bates, T. S., and Coffman, D. J.: VAMOS Ocean-Cloud-Atmosphere-Land Study -
1257 Regional Experiment (VOCALS-REx): Physical, optical, and chemical properties of atmospheric
1258 marine aerosols aboard NOAA R/V Ronald H. Brown in the tropical eastern Pacific, 2008-10-20 to
1259 2008-12-01 (NCEI Accession 0310622). NOAA National Centers for Environmental Information.
1260 [dataset], <https://doi.org/10.25921/maf-2n04>, 2025e.

1261 Quinn, P. K., Bates, T. S., and Coffman, D. J.: The second Aerosol Characterization Experiment (ACE-
1262 2): Physical, optical, and chemical properties of atmospheric marine aerosols aboard IBSS R/V
1263 Vodyanitskiy in the subtropical northeast Atlantic, 1997-06-19 to 1997-07-23 (NCEI Accession
1264 0311148). NOAA National Centers for Environmental Information. [dataset],
1265 <https://doi.org/10.25921/3fk0-0m36>, 2025f.

1266 Quinn, P. K., Bates, T. S., and Coffman, D. J.: Atlantic Tradewind Ocean-Atmosphere Mesoscale
1267 Interaction Campaign (ATOMIC): Physical, optical, and chemical properties of atmospheric marine
1268 aerosols aboard NOAA R/V Ronald H. Brown in the tropical North Atlantic, 2020-01-07 to 2020-02-11
1269 (NCEI Accession 0311369). NOAA National Centers for Environmental Information. [dataset],
1270 <https://doi.org/10.25921/w7ab-3s87>, 2026a.

1271 Quinn, P. K., Bates, T. S., and Coffman, D. J.: Indian Ocean Experiment (INDOEX): Physical, optical,
1272 and chemical properties of atmospheric marine aerosols aboard NOAA R/V Ronald H. Brown in the
1273 Atlantic and Indian Oceans, 1999-01-14 to 1999-03-31 (NCEI Accession 0312108). NOAA National
1274 Centers for Environmental Information. [dataset], <https://doi.org/10.25921/67kx-2d82>, 2026b.

1275 Quinn, P. K., Bates, T. S., and Coffman, D. J.: Pacific Sulfur-Stratus Investigation (PSI): Physical and
1276 chemical properties of atmospheric marine aerosols aboard NOAA R/V Discoverer off the coast of

1277 Washington state, 1991-04-16 to 1991-05-01 (NCEI Accession 0311260), NOAA National Centers for
1278 Environmental Information. [dataset], <https://doi.org/10.25921/44nn-d608>, 2026c.

1279 Quinn, P. K., Bates, T. S., and Coffman, D. J.: Western Atlantic Climate Study (WACS): Physical,
1280 optical, and chemical properties of atmospheric marine aerosols in Georges Bank and the Sargasso Sea
1281 aboard NOAA R/V Ronald H. Brown (2012-08-19 to 2012-08-28) and WHOI R/V Knorr (2014-05-20
1282 to 2014-06-06) (NCEI Accession 0310824). NOAA National Centers for Environmental Information.
1283 [dataset], <https://doi.org/10.25921/tx5t-1e17>, 2026d.

1284 Quinn, P. K., Bates, T. S., and Coffman, D. J.: Dynamics of the Madden-Julian Oscillation (DYNAMO)
1285 Field Campaign: Physical, optical, and chemical properties of atmospheric marine aerosols aboard SIO
1286 R/V Roger Revelle in the equatorial Indian ocean, 2011-10-01 to 2011-12-07 (NCEI Accession
1287 0310825). NOAA National Centers for Environmental Information. [dataset],
1288 <https://doi.org/10.25921/m0ec-rn58>, 2026e.

1289 Quinn, P. K., Bates, T. S., and Coffman, D. J.: Combined Sensor Program (CSP): Physical, optical, and
1290 chemical properties of atmospheric marine aerosols aboard NOAA R/V Discoverer in the central and
1291 tropical western Pacific, 1996-03-15 to 1996-04-12 (NCEI Accession 0311408). NOAA National
1292 Centers for Environmental Information. [dataset], <https://doi.org/10.25921/pgzy-5h08>, 2026f.

1293 Quinn, P. K., Bates, T. S., and Coffman, D. J.: Aerosol Characterization Experiment (ACE-1): Physical,
1294 optical, and chemical properties of atmospheric marine aerosols aboard NOAA R/V Discoverer in the
1295 southern hemisphere, 1995-10-13 to 1995-12-13 (NCEI Accession 0311430). NOAA National Centers
1296 for Environmental Information. [dataset], <https://doi.org/10.25921/z3bm-y330>, 2026g.

1297 Quinn, P. K., Bates, T. S., and Coffman, D. J.: Radiatively Important Trace Species (RITS) Field
1298 Campaign: Physical, optical, and chemical properties of atmospheric marine aerosols aboard NOAA
1299 R/V Surveyor in the central Pacific, 1993-03-20 to 1993-05-08 and 1993-11-21 to 1994-01-08 (NCEI

1300 Accession 0310738). NOAA National Centers for Environmental Information. [dataset],
1301 <https://doi.org/10.25921/ec4p-9410>, 2026h.

1302 Quinn, P. K., Bates, T. S., and Coffman, D. J.: NAURU-99 Field Campaign: Physical, optical, and
1303 chemical properties of atmospheric marine aerosols aboard NOAA R/V Ronald H. Brown in the
1304 southwestern Pacific, 1999-06-14 to 1999-07-16 (NCEI Accession 0311261). NOAA National Centers
1305 for Environmental Information. [dataset], <https://doi.org/10.25921/e2rz-yg88>, 2026i.

1306 Quinn, P. K., Bates, T. S., and Coffman, D. J.: Asian Pacific Regional Aerosol Characterization
1307 Experiment (ACE-Asia): Physical, optical, and chemical properties of atmospheric marine aerosols
1308 aboard NOAA R/V Ronald H. Brown in the western Pacific, 2001-03-15 to 2001-04-20 (NCEI
1309 Accession 0311457). NOAA National Centers for Environmental Information. [dataset],
1310 <https://doi.org/10.25921/jd13-t245>, 2026j.

1311 Quinn, P. K., Bates, T. S., and Coffman, D. J.: Marine Aerosol and Gas Exchange (MAGE-92) Field
1312 Campaign: Physical and chemical properties of atmospheric marine aerosols aboard NOAA R/V John
1313 Vickers in the tropical Pacific, 1992-02-21 to 1992-03-23 (NCEI Accession 0310736). NOAA National
1314 Centers for Environmental Information. [dataset], <https://doi.org/10.25921/bz8f-b917>, 2026k.

1315 Quinn, P. K., Bates, T. S., and Coffman, D. J.: New England Air Quality Study (NEAQS): Physical,
1316 optical, and chemical properties of atmospheric marine aerosols aboard NOAA R/V Ronald H. Brown
1317 in the Gulf of Maine and the northwest Atlantic, 2002-07-12 to 2002-08-10 and 2004-07-05 to 2004-08-
1318 13 (NCEI Accession 0311433). NOAA National Centers for Environmental Information. [dataset],
1319 <https://doi.org/10.25921/q66h-r438>, 2026l.

1320 Quinn, P. K., Bates, T. S., Coffman, D. J., and Covert, D. S.: Influence of particle size and chemistry on
1321 the cloud nucleating properties of aerosols, *Atmospheric Chemistry and Physics*, 8, 1029 - 1042, 2008.

1322 Quinn, P. K., Kapustin, V. N., Bates, T. S., and Covert, D. S.: Chemical and optical properties of marine
1323 boundary layer aerosol particles of the mid-Pacific in relation to sources and meteorological transport,
1324 *Journal of Geophysical Research - Atmosphere*, 101, 6931 - 6951, 1996.

1325 Quinn, P. K., Bates, T. S., Coffman, D. J., Upchurch, L. M., and Johnson, J. E.: Wintertime
1326 observations of tropical northwest Atlantic aerosol properties during ATOMIC: Varying mixtures of
1327 dust and biomass burning, *Journal of Geophysical Research - Atmosphere*, 127, doi:
1328 10.1029/2021JD036253, 2022.

1329 Quinn, P. K., Coffman, D. J., Johnson, J. E., Upchurch, L. M., and Bates, T. S.: Small fraction of
1330 marine cloud condensation nuclei made up of sea spray aerosol, *Nature Geoscience*, 10, 674 - 679,
1331 2017.

1332 Quinn, P. K., Coffman, D. J., Kapustin, V. N., Bates, T. S., and Covert, D. S.: Aerosol optical properties
1333 in the MBL during ACE-1 and the underlying chemical and physical aerosol properties, *Journal of*
1334 *Geophysical Research - Atmosphere*, 103, 16,547 - 516,564, 1998b.

1335 Quinn, P. K., Collins, D. B., Grassian, V. H., Prather, K. A., and Bates, T. S.: Chemistry and related
1336 properties of freshly emitted sea spray aerosol, *Chemical Reviews*, doi:10.1021/cr500713g, 2015.

1337 Quinn, P. K., Marshall, S., Bates, T. S., Covert, D. S., and Kapustin, V. N.: Comparison of measured
1338 and calculated aerosol properties relevant to the direct radiative forcing of tropospheric sulfate aerosol
1339 particles, *Journal of Geophysical Research - Atmospheres*, 100, 8977 - 8992, 1995.

1340 Quinn, P. K., Covert, D. S., Bates, T. S., Kapustin, V. N., Ramsey-Bell, D. C., and McInnes, L. M.:
1341 Dimethylsulfide/cloud condensation nuclei/climate system: Relevant size-resolved measurements of the
1342 chemical and physical properties of atmospheric aerosol particles, *Journal of Geophysical Research -*
1343 *Atmosphere*, 98, 10,411 - 410,4227, 1993.

- 1344 Quinn, P. K., Bates, T. S., Schultz, K. S., Coffman, D. J., Frossard, A. A., Russell, L. M., Keene, W. C.,
1345 and Kieber, D. J.: Contribution of sea surface carbon pool to organic matter enrichment in sea spray
1346 aerosol, *Nature Geoscience*, 7, 228-232, 10.1038/ngeo2092, 2014.
- 1347 Quinn, P. K., Coffman, D. J., Bates, T. S., Miller, T. L., Johnson, J. E., Voss, K. J., Welton, E. J., and
1348 Neusüß, C.: Dominant aerosol chemical components and their contribution to extinction during the
1349 Aerosols99
1350 cruise across the Atlantic, *Journal of Geophysical Research - Atmosphere*, 106, 720,783 - 720,809, 2001.
- 1351 Quinn, P. K., Bates, T. S., Coffman, D. J., Upchurch, L. M., Moore, R., Ziemba, L., Bell, T., Saltzman,
1352 E. S., et al.: Seasonal variations in western North Atlantic remote marine aerosol properties, *Journal of*
1353 *Geophysical Research - Atmosphere*, 124, 214,240 - 214,261, 2019.
- 1354 Quinn, P. K., Bates, T. S., Miller, T. L., Coffman, D. J., Johnson, J. E., Harris, J. M., Ogren, J., Forbes,
1355 G., et al.: Surface submicron aerosol chemical composition: What fraction is not sulfate?, *Journal of*
1356 *Geophysical Research - Atmospheres*, 105, 6785 - 6805, 2000.
- 1357 Quinn, P. K., Bates, T. S., Baynard, T., Clarke, A., Onasch, T. B., Wang, W., Rood, M. J., Andrews, E.,
1358 et al.: Impact of particulate organic matter on the relative humidity dependence of light scattering: A
1359 simplified parameterization, *Geophysical Research Letters*, 32, doi:10.1029/2005GL024322, 2005b.
- 1360 Quinn, P. K., Bates, T. S., Coffman, D. J., Onasch, T. B., Worsnop, D. R., Baynard, T., de Gouw, J. A.,
1361 Goldan, P. D., et al.: Impacts of sources and aging on submicrometer aerosol properties in the marine
1362 boundary layer across the Gulf of Maine, *Journal of Geophysical Research - Atmosphere*, 111,
1363 doi:10.1029/2006JD007582, 2006.
- 1364 Quinn, P. K., Thompson, E. J., Coffman, D. J., Baidar, S., Bariteau, L., Bates, T. S., Bigorre, S.,
1365 Brewer, A., et al.: Measurements from the RV Ronald H. Brown and related platforms as part of the

- 1366 Atlantic Tradewind Ocean-Atmosphere Mesoscale Interaction Campaign (ATOMIC), Earth System
1367 Science Data, 13, 1759 - 1790, 2021.
- 1368 Raes, F., Bates, T. S., McGovern, F., and Vanliedekerke, M.: The Second Aerosol Characterization
1369 Experiment, *Tellus*, 52B, 111 - 125, 2000.
- 1370 Ramanathan and al., e.: Indian Ocean Experiment: An integrated analysis of the climate forcing effects
1371 of the great Indo-Asian haze, *Journal of Geophysical Research - Atmospheres*, 106, 28,371 - 328,398,
1372 2001.
- 1373 Reddington, C. L., Carslaw, K. S., Stier, P., Schutgens, N., Coe, H., Liu, D., Allan, J., Browse, J., et al.:
1374 The Global Aerosol Synthesis and Science Project (GASSP), *Bulliten of the American Meteorology*
1375 *Society*, 98, 1857 - 1877, 2017.
- 1376 Reineking, A. and Porstendorfer, J.: Measurements of particle loss functions in a differential mobility
1377 analyzer for different flow rates, *Aerosol Science and Technology*, 5, 483 - 487, 1986.
- 1378 Roberts, G. C. and Nenes, A.: A continuous-flow streamwise thermal-gradient CCN chamber for
1379 atmospheric measurements, *Aerosol Science and Technology*, 39, 206 - 221, 2005.
- 1380 Russell, L. M., Hawkins, L. N., Frossard, A. A., Quinn, P. K., and Bates, T. S.: Carbohydrate-like
1381 composition of submicron atmospheric particles and their production from ocean bubble bursting,
1382 *Proceedings of the National Academy of Sciences*, 107, 6652 - 6657, 2010.
- 1383 Russell, P. B., Livingston, J. M., Redemann, J., Schmid, B., Ramirez, S. A., Eilers, J., Kahn, R., Chu, D.
1384 A., et al.: Multi-grid-cell validation of satellite aerosol property retrievals in INTEX/ITCT/ICARTT
1385 2004, *Journal of Geophysical Research - Atmosphere*, 112, doi:10.1029/2006JD007606, 2007.

1386 Russell, P. B., Redemann, J., Schmid, B., Bergstrom, R. W., Livingston, J. M., McIntosh, D. M.,
1387 Ramirez, S. A., Hartley, S. A., et al.: Comparison of aerosol single scattering albedos derived by diverse
1388 techniques in two North Atlantic experiments, *Journal of Atmospheric Science*, 59, 609 - 619, 2002.

1389 Ryerson, T. B., Andrews, A. E., Angevine, W. M., Bates, T. S., Brock, C. A., Cairns, B., Cohen, R. C.,
1390 Cooper, O. R., et al.: The 2010 California Research at the Nexus of Air Quality and Climate Change
1391 (CalNex) field study, *Journal of Geophysical Research - Atmospheres*, 118, 10.1002/jgrd.50331, 2013.

1392 Savoie, D. L. and Prospero, J. M.: Water-soluble potassium, calcium, and magnesium in the aerosols
1393 over the tropical North Atlantic, *Journal of Geophysical Research - Atmosphere*, 85, 385 - 392, 1980.

1394 Schauer, J. J., Mader, B. T., DeMinter, J. T., Heidemann, G., Bae, M. S., Seinfeld, J. H., Flagan, R. C.,
1395 Cary, R. A., et al.: ACE-Asia intercomparison of a thermal-optical method for the determination of
1396 particle-phase organic and elemental carbon, *Environmental Science and Technology*, 37,
1397 10.1021/es020622f, 2003.

1398 Seinfeld, J. H.: *Atmospheric chemistry and physics of air pollution*, John Wiley 1986.

1399 Shaw, G. E.: Sun Photometry, *Bulliten of the American Meteorology Society*, 64, 4 - 9, 1983.

1400 Smirnov, A., Holben, B. N., Slutsker, I., Giles, D. M., McClain, C. R., Eck, T. F., Sakerin, S. M.,
1401 Macke, A., et al.: Maritime aerosol network as a component Aerosol Robotic Network, *Journal of*
1402 *Geophysical Research - Atmosphere*, 114, doi: 10.1029/2008JD011257, 2009.

1403 Solarzano, L.: Determination of ammonia in natural waters by the phenolhypochorite method,
1404 *Limnology and Oceanography*, 14, 799 - 801, 1969.

1405 Stevens, B., Bondy, S., Farrell, D., Ament, F., Blyth, A., Fairall, C. W., Karstensen, F., Quinn, P. K., et
1406 al.: EUREC4A, *Earth System Science Data*, 13, 4067-4119, 2021.

1407 Swietlicki, E., Hannsson, H.-C., Hameri, K., Svenningsson, B., Massling, A., Mcfiggans, G., McMurry,
1408 P. H., Petaja, T., et al.: Hygroscopic properties of submicrometer atmospheric aerosol particles
1409 measured with H-TDMA instruments in various environments - A review, *Tellus*, 60B, 432 - 469, 2008.

1410 Turpin, B. J. and Lim, H.: Species contribution to PM_{2.5} concentrations: Revisiting common
1411 assumptions for estimating organic mass, *Aerosol Science and Technology*, 35, 602 - 610, 2001.

1412 Uno, I., Satake, S., Carmichael, G. R., Tang, Y., Wang, Z., Takemura, T., Sugimoto, N., Shimizu, A., et
1413 al.: Numerical study of Asian dust transport during the springtime of 2001 simulated with the CFORS
1414 model, *Journal of Geophysical Research - Atmosphere*, 109, doi: 10.1029/2003JD004222, 2004.

1415 Virkkula, A., Ahlquist, N. C., Covert, D. S., Arnott, W. P., Sheridan, P. J., Quinn, P. K., and Coffman,
1416 D. J.: Modification, Calibration and a Field Test of an Instrument for Measuring Light Absorption by
1417 Particles, *Aerosol Science and Technology*, 39, 68 - 83, 2005.

1418 Voss, K. J., Welton, E. J., Quinn, P. K., Johnson, J. E., Thompson, A. M., and Gordon, H. R.: Lidar
1419 measurements during Aerosols99, *Journal of Geophysical Research - Atmosphere*, 106,
1420 10.1029/2001JD900217, 2001.

1421 Wang, H. C. and John, W.: Particle density correction for the aerodynamic particle sizer, *Aerosol*
1422 *Science and Technology*, 6, 191 - 198, 1987.

1423 Wang, J., Christopher, S. A., Brechtel, F. J., Kim, J., Schmid, B., Redemann, J., Russell, P. B., Quinn,
1424 P. K., and Holben, B. N.: Geostationary satellite retrievals of aerosol optical thickness during ACE-
1425 Asia, *Journal of Geophysical Research - Atmosphere*, 108, 10.1029/2003JD003580, 2003.

1426 Wang, J., Flagan, R. C., Seinfeld, J. H., Jonsson, H. H., Collins, D. R., Russell, P. B., Schmid, B.,
1427 Redemann, J., et al.: Clear-column radiative closure during ACE-Asia: Comparison of multiwavelength

1428 extinction derived from particle size and composition with results from Sun photometry, Journal of
1429 Geophysical Research - Atmosphere, 107, <https://doi.org/10.1029/2002JD002465>, 2002.

1430 Weber, R. J., Orsini, D., Daun, Y., Lee, Y.-N., Klotz, P. J., and Brechtel, F. J.: A particle-into-liquid
1431 collector for rapid measurement of aerosol bulk chemical composition, Aerosol Science and
1432 Technology, 35, 718 - 727, 2001.

1433 Welton, E. J., Voss, K. J., Quinn, P. K., Flatau, P. J., Markovic, M. Z., Campbell, J. R., Spinhirne, J. D.,
1434 Gordon, H. R., and Johnson, J. E.: Measurements of aerosol vertical profiles and optical properties
1435 during INDOEX 1999 using micropulse lidars, Journal of Geophysical Research - Atmosphere, 107,
1436 10.1029/2000JD000038, 2002.

1437 Whittlestone, S. and Zahorowski, W.: Baseline radon detectors for shipboard use: Development and
1438 deployment in the First Aerosol Characterization Experiment (ACE 1), Journal of Geophysical
1439 Research - Atmosphere, 103, 16743 - 16751, 1998a.

1440 Whittlestone, S., Gras, J., and Siems, S. T.: Surface air mass origins during the First Aerosol
1441 Characterization Experiment (ACE-1), Journal of Geophysical Research - Atmosphere, 103, 16,341 -
1442 316,350, 1998b.

1443 Wiedensohler, A., Orsini, D., Covert, D. S., Coffman, D. J., Cantrell, W., Havlicek, M., Brechtel, F. J.,
1444 Russell, L. M., et al.: Intercomparison study of size dependent counting efficiency of 26 condensation
1445 particle counters, Aerosol Science and Technology, 27, 224 - 242, 1997.

1446 Witek, M., Flatau, P. J., Quinn, P. K., and Westphal, D. L.: Global sea-salt modeling: Results and
1447 validation against multicampaign shipboard measurements, Journal of Geophysical Research -
1448 Atmosphere, 112, doi:10.1029/2006JD007779, 2007.

- 1449 Wood, R., Mechoso, C. R., Bretherton, C. S., Weller, R. A., Huebert, B. J., Straneo, F., Albrecht, B. A.,
1450 Coe, H., et al.: The VAMOS Ocean-Cloud-Atmosphere-Land Study Regional Experiment (VOCALS-
1451 REx): goals, platforms, and field operations, *Atmospheric Chemistry and Physics*, 11, 627 - 654, 2011.
- 1452 Yoneyama, K., Zhang, C., and Long, C. N.: Tracking pulses of the Madden-Julian Oscillation, *Bulliten*
1453 *of the American Meteorological Society*, 94, 1871 - 1891, 2013.
- 1454 Young, J. F.: Humidity control in the laboratory using salt solutions, *Journal of Applied Chemistry*, 17,
1455 241 - 245, 1967.
- 1456 Zang, Z. and Liu, B. Y. H.: Performance of the TSI 3760 condensation nuclei counter at reduced
1457 pressures and flow rates, *Aerosol Science and Technology*, 15, 228 - 238, 1991.
- 1458